

Study of $\pi N \rightarrow \pi\pi N$ processes on polarized targets: Quantum environment and its dephasing interaction with particle scattering

Miloslav Svec*

Physics Department, Dawson College, Montreal, Quebec H3Z 1A4, Canada
(Received 6 May 2013; published 6 April 2015)

Unitary evolution law describes isolated particle scattering processes in an empty Minkowski spacetime. We put forward a hypothesis that the physical Universe includes a quantum environment that interacts with some particle scattering and decay processes. While the scattering process is governed by the S -matrix dynamics and its conservation laws and unitarity, the interaction with the environment evolves the produced final state $\rho_f(S)$ to the observed state $\rho_f(O)$. To be consistent with the Standard Model this new interaction must be a pure dephasing interaction. Governed by a nonunitary evolution law, it modifies the phases of the S -matrix amplitudes and can give rise to mixing of such amplitudes to form observed amplitudes. We present the first test of unitary evolution law in particle scattering. Conservation of P -parity in strong interactions imposes constraints on partial wave helicity and nucleon transversity amplitudes in $\pi N \rightarrow \pi\pi N$ processes. An independent set of constraints on these amplitudes is imposed by the S -matrix unitary evolution law. The unitary evolution evolves pure initial states into pure final states leading to 9 independent constraints on 16 components of angular intensities in $\pi N \rightarrow \pi\pi N$ processes. When expressed in terms of parity conserving transversity amplitudes, all 9 constraints are identities provided a single constraint on the transversity amplitudes holds true. The constraint implies that relative phases between transversity amplitudes of the same naturality and transversity must be 0 or $\pm\pi$. Assuming a self-consistent set of these unitary phases we use the CERN data on spin observables R_u^0 and R_y^0 to determine a unique solution for the S - and P -wave moduli below 1080 MeV. The data require $\rho^0(770) - f_0(980)$ mixing in the S -wave but this unitary solution is excluded by data on observables R_x^0 within at least 5 standard deviations. All previous amplitude analyses of $\pi N \rightarrow \pi\pi N$ processes found nonunitary relative phases in an apparent violation of the unitary evolution law. The contrast between the predicted unitary relative phases and the observed nonunitary phases presents unambiguous evidence for the nonunitary evolution of the produced final state and supports the hypothesis of the existence of a quantum environment and its pure dephasing interaction with particle scattering processes.

DOI: 10.1103/PhysRevD.91.074005

PACS numbers: 13.85.Hd, 13.88.+e

I. INTRODUCTION

The concept of the S -matrix is deeply rooted in the concept of Minkowski spacetime and its Poincaré symmetry. The Poincaré group on the Minkowski spacetime allows us to define particle four-momentum and spin. This in turn allows us to consider particle scattering and decay of incident states into outgoing states. The resulting probability amplitudes are summarized as S -matrix elements. The conservation of probability imposes unitarity of the S -matrix. The S -matrix commutes with the generators of the Poincaré group. As a result of this symmetry the total four-momentum and total angular momentum are conserved in particle scattering and decays. Internal symmetries of the S -matrix impose additional conservation laws.

In S -matrix theory particle scattering and decays are isolated and time-reversible quantum events in Minkowski spacetime. The reason for this is that Minkowski spacetime is empty. There is no quantum environment in Minkowski spacetime with which the scattering and decay processes

could interact. Another reason is that the scattering and decay processes do not interact with the Minkowski spacetime itself since it has no quantum structure that, in effect, could present itself as a quantum environment.

Particle scattering and decay processes take place, in fact, in the real physical Universe. Suppose that there exists a quantum environment in the Universe that interacts with particle processes. Such an interaction cannot originate in the known interactions of the Standard Model. These interactions would lead to observable violation of the conservation laws and render the dynamics of particle interaction inaccessible to experiment. The interaction of particle processes with the quantum environment must originate from the outside of the Standard Model. If the quantum environment and this new kind of interaction are to be an integral part of nature, then they must be fully consistent with the conservation laws and unitarity of the Standard Model.

There exists such an interaction in nature. It is the pure dephasing interaction between a quantum system S and a quantum environment E which is a nondissipative interaction that affects only the phase(s) of the quantum system

*svec@hep.physics.mcgill.ca

S . In general, its effect is to change the quantum information content of the quantum system S . Unlike the force of gravity, which has undetectable effects on particle processes, the pure dephasing interaction could be observable. The key to observing the dephasing interaction, and thus the quantum environment, is the S -matrix unitarity.

The evolution of an isolated initial state ρ_i into isolated final states $\rho_f(S)$ is governed by the unitary evolution law

$$\rho_f(S) = S\rho_i S^\dagger. \quad (1.1)$$

Evolution of an initial state ρ_i interacting with a quantum environment E is governed by a nonunitary evolution law given by Kraus representation

$$\rho_f(A) = \sum_k A_k \rho_i A_k^\dagger \quad (1.2)$$

where A_k are unitary or nonunitary Kraus operators [1–4]. The necessary and sufficient condition for the nonunitary evolution law to be consistent with the unitary evolution law is that the interaction with the environment be a final state interaction which involves only the produced state $\rho_f(S)$. The nonunitary evolution of the S -matrix final state $\rho_f(S)$ yields the observed nonunitary final state $\rho_f(O)$

$$\rho_f(O) = \sum_k A_k \rho_f(S) A_k^\dagger. \quad (1.3)$$

The effect of the pure dephasing interaction with the environment thus shall be to modify the phases of the S -matrix amplitudes in the observed amplitudes of the new state $\rho_f(O)$. The existence of the quantum environment will manifest itself in the difference between the phases of the observed and S -matrix amplitudes. To an observer (initially) unaware of the nonunitary evolution of the produced final state $\rho_f(S)$ this difference would appear as an apparent violation of the unitary evolution law. An observer who insists on the validity of the unitary evolution law would explain the difference differently: there is a presence of a short time scale in which Standard Model interactions act to produce the S -matrix final state $\rho_f(S)$ and afterwards a nonunitary evolution of this state leaves its imprints on the observed final state $\rho_f(O)$.

To gain information about the phases of the S -matrix amplitudes we shall use the fact that the S -matrix unitary evolution law evolves pure initial states ρ_i into pure final states $\rho_f(S)$ in exclusive processes. In two-body processes such as $\pi N \rightarrow \pi N$ this condition imposes no constraints on the amplitudes and thus no specific information about their phases. The situation is different in $\pi N \rightarrow \pi\pi N$ and similar production processes.

In this work we aim to test the unitary evolution law in the pion production $\pi^- p \rightarrow \pi^- \pi^+ n$ measured at CERN on polarized target at 17.2 GeV/c [5]. We develop the

necessary spin formalism and show that the purity of the final state density matrix in $\pi N \rightarrow \pi\pi N$ processes is controlled by the recoil nucleon polarization. Evolution of pure initial states to pure final states imposes 9 constraints on 16 angular intensities describing the final state. Using P -parity conservation we show that all constraints are identities provided that the partial wave amplitudes satisfy the conditions

$$\text{Im}(U_{\lambda\tau}^J N_{\mu-\tau}^{K*}) = 0 \quad (1.4)$$

where $U_{\lambda\tau}^J$ and $N_{\mu-\tau}^K$ are parity conserving nucleon transversity unnatural and natural exchange amplitudes with dipion spin, helicity and nucleon transversity J, λ, τ and $K, \mu, -\tau$, respectively. The conditions (1.4) imply that the relative phases between any two unnatural or two natural exchange amplitudes of the same transversity τ as well as between any unnatural and natural exchange amplitudes of opposite transversities must be 0 or $\pm\pi$. As a result, the unnatural and natural amplitudes share a common phase $\Phi(U_{0\tau}^0)$ and $\Phi(N_{1\tau}^1)$, respectively. Because strong, electromagnetic and weak interactions do not mix particles with different spins, self-consistency requires that there be no mixing of resonances of different spins in any partial wave amplitudes with such unitary phases.

The elegant simplicity and uniqueness of these predictions render the test of unitary evolution law possible using the existing CERN measurements on polarized target at dipion masses below 1080 MeV where S - and P -wave amplitudes dominate. We found that the measurements of density matrices R_u^0 and R_v^0 yield a solution with $\rho^0(770) - f_0(980)$ mixing in the S -wave. But this solution is entirely excluded by the measured data on density matrix R_x^0 within at least five standard deviations. This result shows that the data require $\rho^0(770) - f_0(980)$ mixing in the S -wave but reject unitary phases in an apparent violation of the unitary evolution law.

All previous amplitude analyses of $\pi^- p \rightarrow \pi^- \pi^+ n$ at 17.2 GeV/c [6–15] and at 1.78 GeV/c [16] as well as of $\pi^+ n \rightarrow \pi^+ \pi^- p$ at 5.98 and 11.85 GeV/c [10–12] found nonunitary relative phases of all transversity amplitudes. Recent amplitude analysis of the S - and P -wave subsystem in $\pi^- p \rightarrow \pi^- \pi^+ n$ at 17.2 GeV/c established that the width of the $\rho^0(770)$ resonance peak observed in all P -wave amplitudes does not depend on its helicity λ [13,15] as required by the rotational/Lorentz symmetry of the S -matrix. Furthermore, the nonunitary relative phases of the S - and P -wave amplitudes are near the unitary values. These findings show that the observed nonunitary phases are consistent with the S -matrix unitary evolution law for the production process. This is possible if the nonunitary phases arise from a pure dephasing interaction of the produced S -matrix final state $\rho_f(S)$ with a quantum environment. The contrast between the predicted unitary relative phases and the observed nonunitary phases

therefore presents unambiguous evidence for the nonunitary evolution of the produced final state and supports the hypothesis of the existence of the quantum environment and its pure dephasing interaction with particle scattering processes.

In a sequel paper [17] we show that the consistency of the pure dephasing interaction with the Standard Model in $\pi N \rightarrow \pi\pi N$ processes requires that it be a dipion spin mixing interaction the effect of which is the mixing of S -matrix partial wave amplitudes to form observable amplitudes. The theory predicts $\rho^0(770) - f_0(980)$ mixing in the S - and P -wave amplitudes in $\pi^- p \rightarrow \pi^- \pi^+ n$. The predicted moduli and relative phases of the mixed amplitudes are in an excellent qualitative agreement with the experimental results [13,15]. The evidence for $\rho^0(770) - f_0(980)$ mixing dates back to the 1960s [18–23] and was later confirmed in all amplitude analyses of $\pi^- p \rightarrow \pi^- \pi^+ n$ and $\pi^+ n \rightarrow \pi^+ \pi^- p$ on polarized targets. A survey of evidence for $\rho^0(770) - f_0(980)$ mixing from all these amplitude analyses on polarized targets is presented in Ref. [24].

The issue of the experimental test of the unitary evolution law was first raised in 1974 by Marinov who suggested to describe the time evolution of the $K^0\bar{K}^0$ system using a model of a nonunitary evolution from pure states into mixed states [25]. He found that such evolution is time irreversible and violates CPT symmetry and proposed to make a complete measurement of matrix elements of ρ_f to test the unitary evolution law. In 1980 Wald showed rigorously that any scattering process of particles that evolves a pure initial state into a mixed final state is not an invertible process and therefore it is time irreversible and violates CPT symmetry [26]. He suggested that such nonunitary processes will occur in curved spacetime, and that quantum gravity violates CPT symmetry and time-reversal invariance. In 1982 Hawking pointed out that particle scattering does not take place in a structureless continuum of the Minkowski spacetime but in an environment of quantum spacetime fluctuations and suggested that pure initial states of interacting particles will evolve into mixed final states due to the interaction of the particle scattering process with quantum fluctuations of the spacetime metric—at any energy [27,28]. Hawking questioned the universal validity of the unitary time evolution in the presence of metric fluctuations, and suggested that initial and final state density matrices ρ_i and ρ_f are connected by a nonunitary evolution law described by a linear but nonunitary and noninvertible superscattering operator

$$\rho_f = \rho_i. \quad (1.5)$$

To avoid negative probabilities the mapping (1.5) must be completely positive. A linear mapping (1.5) is completely positive if and only if it has the form of the Kraus representation (1.2) [1–4]. Recently Unruh and Wald

[29] and Oppenheim and Reznik [30] demonstrated the feasibility of nonunitary evolution in quantum field theories. However, in these models Lorentz invariance fails. In 2002 Greenberg showed that any interacting (scattering producing) theory that violates CPT invariance necessarily violates Lorentz invariance [31].

Hawking's ideas inspired attempts to test unitary evolution law experimentally. The efforts focused mainly on nonunitary time evolution of the neutral kaon $K^0\bar{K}^0$ system using Lindblad-type evolution laws [32–37] and led to the predictions of CPT violation and a modification of Einstein-Podolsky-Rosen correlations [38,39]. During the recent years experiments with neutral kaons have yielded sensitive results on violations of CPT symmetry, time-reversal invariance and entanglement of kaon pairs [40–42]. So far these experiments did not provide a conclusive confirmation of a nonunitary evolution of free neutral kaon systems. These observations can be understood as the result of the absence of the diparticle spin mixing in the time evolution of the $K^0\bar{K}^0$ system.

What are the implications of the nonunitary evolution for the CPT symmetry in $\pi N \rightarrow \pi\pi N$ processes? In quantum field theory and in the Standard Model CPT symmetry is conserved as a consequence of locality, Lorentz symmetry and a Hermitian interaction Lagrangian [43,44]. This means that the produced final state $\rho_f(S)$ and the S -matrix amplitudes are CPT symmetric. According to Wald's theorem nonunitary evolution of $\rho_f(S)$ to the observed state $\rho_f(O)$ violates CPT symmetry and is time irreversible. Greenberg's theorem then implies a violation of Lorentz symmetry. This means that the nonunitary evolution and pure dephasing interaction cannot be described by local and Lorentz invariant quantum field theory. In Ref. [17] we show that the Kraus operators are forward scattering operators akin to forward scattering of light in a refracting medium. The forward scattering of dipion spin states on recoil nucleon into dipion spin states with different spin leads to dephasing and spin mixing of the S -matrix amplitudes to form the observed amplitudes.

Interactions that are invariant under CPT symmetry lead to observables that are invariant under CPT as well. Conversely, interactions that violate CPT symmetry lead to observables that violate CPT symmetry. It is important to recognize that the CPT violating nonunitary evolution and interaction with the quantum environment do not contradict the CPT invariant interactions and their observables involved in the production of the state $\rho_f(S)$. Thus we may expect e.g. the masses and lifetimes of π^- and π^+ to be the same and rotationally invariant width and mass of the $\rho(770)$ resonance in $\pi^- p \rightarrow \pi^- \pi^+ n$. The CPT violating interactions will manifest themselves in other observable aspects of the pion creation process. In this case the CPT violating observables are the observed transversity amplitudes. The distinct CPT violating effects seen only in these nonunitary amplitudes are their nonunitary phases and the

spin mixing. As an alternative to spin mixing certain observed amplitudes violate the so called cosine gap condition which S -matrix amplitudes must satisfy [17].

The paper is organized as follows. In Sec. II we briefly discuss the evolution of pure initial states by unitary and nonunitary evolution laws. In Sec. III we show that S -matrix unitary evolution implies evolution from pure initial states into pure final states in exclusive processes. In Secs. IV–VI we review and develop the spin formalism necessary to derive and discuss the constraints imposed by the unitary evolution law on the nucleon transversity amplitudes. We emphasize the coherent superposition of diparticle states and the constraints imposed by the conservation of P -parity on partial wave amplitudes. The final state density matrix is defined and its properties derived in some detail. This material will be used also in the sequel paper. In Sec. VII we present the unitary constraints on angular intensities from which we derive the unitary condition (1.4) and a self-consistent set of unitary phases. In Sec. VIII we present a unique unitary solution for S - and P -amplitudes below 1080 MeV and show it is excluded by the data on observables R_x^0 . This conclusion does not change when we include D -waves in the analysis. We discuss the evidence for the quantum environment and the dephasing interaction in Sec. IX and a physical interpretation of the unitary and nonunitary relative phases in Sec. X. We present our conclusions and outlook in Sec. XI. The Appendix provides an outline of the proof of the unitary condition (1.4).

II. UNITARY AND NONUNITARY EVOLUTION LAWS

Let H be a Hilbert space of vector states with an orthonormal basis $|n\rangle, n = 1, N$ where $N = \dim H$. Let $\mathcal{B}(H)$ be the Hilbert-Schmidt space of linear operators on H with an orthonormal basis $|n\rangle\langle m|, n, m = 1, N$. The density matrix $\rho \in \mathcal{B}(H)$ is a Hermitian and positive operator $\rho = \sum \rho_{mn} |m\rangle\langle n|$ with $\text{Tr}(\rho) = 1$. The density matrix ρ represents a pure state if it satisfies the condition $\text{Tr}(\rho^2) = (\text{Tr}(\rho))^2$. A quantum state satisfies this purity condition if and only if its density matrix has the form $\rho = |\Psi\rangle\langle\Psi|$ where $|\Psi\rangle$ is a vector in H .

Let A be a linear operator on H and ρ_i an arbitrary density matrix in $\mathcal{B}(H)$. Then A defines a mapping—or an evolution law—of the state ρ_i into a state ρ_f

$$\rho_f = A\rho_i A^\dagger. \quad (2.1)$$

Let $\rho_i = |i\rangle\langle i|$ be a pure state and $A|i\rangle = |\Psi_A(i)\rangle$. Then $\rho_f = A|i\rangle\langle i|A^\dagger = |\Psi_A(i)\rangle\langle\Psi_A(i)|$ is also a pure state. If A is a unitary operator the mapping is a trace conserving and invertible unitary evolution. Otherwise it is a simple nonunitary evolution with normalized density matrix $\rho'_f = \rho_f / \text{Tr}(\rho_f)$.

To be physically meaningful the mappings from initial to final states must preserve the positivity of all probabilities which requires that they be completely positive. The necessary and sufficient condition for an evolution law to be completely positive is that it has the form called Kraus representation [1–4]

$$\rho_f = \sum_k A_k \rho_i A_k^\dagger \quad (2.2)$$

where A_k are unitary or nonunitary Kraus operators. For trace preserving evolution they satisfy the completeness relation

$$\sum_k A_k^\dagger A_k = I. \quad (2.3)$$

Kraus representation (2.2) describes a general completely positive, nonunitary and noninvertible evolution. Let $\rho_i = |i\rangle\langle i|$ be a pure initial state. Then the final state is a mixed state

$$\rho_f = \sum_k A_k |i\rangle\langle i| A_k^\dagger = \sum_k |\Psi_{A_k}(i)\rangle\langle\Psi_{A_k}(i)|. \quad (2.4)$$

A special case of (2.2) is the evolution law (2.1) which evolves pure initial states into pure final states. It describes evolution of isolated quantum systems while the Kraus representation describes a nonunitary evolution of open quantum systems. Kraus representation arises from a unitary evolution law governing the coevolution of the quantum system with its quantum environment after the interacting degrees of freedom between the two systems have been traced out in their joint final state density matrix [1–4]. The dissipative dephasing interactions exchange not only phases but also four-momentum and/or angular momentum. There is no exchange of four-momentum and/or angular momentum in pure dephasing interactions of the quantum system with its quantum environment.

III. EVOLUTION FROM PURE INITIAL STATES INTO PURE FINAL STATES IN EXCLUSIVE PROCESSES

The unitary S -matrix evolves an arbitrary initial state ρ_i into a final state

$$\rho = S\rho_i S^\dagger. \quad (3.1)$$

Any pure initial state ρ_i can be written in the form $\rho_i = |i\rangle\langle i|$. The evolution operator S brings the state vector $|i\rangle$ to a state vector $|\Psi\rangle = S|i\rangle$ so that $\rho = |\Psi\rangle\langle\Psi|$ is a pure state. Using a completeness relation

$$\sum_f \sum_{\chi_f} \int d\Phi_f |p_f, \chi_f, \gamma_f\rangle\langle p_f, \chi_f, \gamma_f| = I \quad (3.2)$$

the state vector $|\Psi\rangle$ has an explicit form

$$|\Psi\rangle = \sum_f \sum_{\chi_f} \int d\Phi_f |p_f, \chi_f, \gamma_f\rangle \langle p_f, \chi_f, \gamma_f | S | i \rangle \quad (3.3)$$

where the first sum is over all allowed final states f , the second sum is over final state spins χ_f and the integration is over the entire phase space of final state momenta p_f . The

symbol γ_f labels the quantum numbers of the state f . The density matrix $\rho = |\Psi\rangle\langle\Psi|$ has an explicit form

$$\rho = \sum_f \rho_f + \sum_{f'} \sum_{f'' \neq f'} \rho_{f' f''} \quad (3.4)$$

where

$$\begin{aligned} \rho_f &= \sum_{\chi'_f, \chi''_f} \int d\Phi'_f d\Phi''_f \langle p'_f, \chi'_f, \gamma_f | S | i \rangle \langle i | S^+ | p''_f, \chi''_f, \gamma_f \rangle | p'_f, \chi'_f, \gamma_f \rangle \langle p''_f, \chi''_f, \gamma_f | \\ \rho_{f' f''} &= \sum_{\chi'_{f'}, \chi''_{f''}} \int d\Phi_{f'} d\Phi_{f''} \langle p_{f'}, \chi_{f'}, \gamma_{f'} | S | i \rangle \langle i | S^+ | p_{f''}, \chi_{f''}, \gamma_{f''} \rangle | p_{f'}, \chi_{f'}, \gamma_{f'} \rangle \langle p_{f''}, \chi_{f''}, \gamma_{f''} |. \end{aligned} \quad (3.5)$$

The density matrix ρ_f of the final state f is the block-diagonal submatrix of ρ . It is a pure state $\rho_f = |\Psi_f\rangle\langle\Psi_f|$ where

$$|\Psi_f\rangle = \sum_{\chi_f} \int d\Phi_f |p_f, \chi_f, \gamma_f\rangle \langle p_f, \chi_f, \gamma_f | S | i \rangle. \quad (3.6)$$

The projection of ρ_f into a state $\rho_f(p_f)$ with definite final state momenta p_f is given by

$$\begin{aligned} \rho_f(p_f) &= |p_f, \gamma_f\rangle \langle p_f, \gamma_f | \rho | p_f, \gamma_f \rangle \langle p_f, \gamma_f | \\ &= \sum_{\chi'_f, \chi''_f} \langle p_f, \chi'_f, \gamma_f | S | i \rangle \\ &\quad \times \langle i | S^+ | p_f, \chi''_f, \gamma_f \rangle | p_f, \chi'_f, \gamma_f \rangle \langle p_f, \chi''_f, \gamma_f|. \end{aligned} \quad (3.7)$$

It is a pure state $\rho_f(p_f) = |\Psi_f(p_f)\rangle\langle\Psi_f(p_f)|$ where

$$|\Psi_f(p_f)\rangle = \sum_{\chi_f} |p_f, \chi_f, \gamma_f\rangle \langle p_f, \chi_f, \gamma_f | S | i \rangle. \quad (3.8)$$

Note that $\sum_f \int d\Phi_f |p_f, \gamma_f\rangle \langle p_f, \gamma_f| = I$ since the spin projection operators $\sum_{\chi_f} |\chi_f\rangle\langle\chi_f| = I$. The S -matrix unitary evolution (3.1) and the completeness relation (3.2) thus imply that for any initial pure state ρ_i all final states $\rho_f(p_f)$ must be pure states.

IV. TWO-PARTICLE COHERENT STATES AND DIPARTICLES

The state vector $|p_1 p_2; \mu_1 \mu_2; \gamma\rangle$ of two noninteracting particles with four-momenta p_1, p_2 , helicities μ_1, μ_2 and quantum numbers γ is a direct product of two single-particle helicity states. It is an eigenstate of the momentum operator P_μ with eigenvalue $p = p_1 + p_2$ and invariant mass $m^2 = p^2$. It does not define an irreducible

representation of the restricted inhomogeneous Lorentz group, and therefore it has no definite spin and P -parity. However, it can be expressed as a coherent superposition of spin states with four-momentum p and definite spin and parity. These states have a character of free noninteracting single-particle helicity states with variable mass and carry the quantum numbers γ . We shall refer to these states as diparticles.

In the center-of-mass system where $\vec{p}^* = \vec{p}_1^* + \vec{p}_2^* = 0$ and $E^* = m$ the two-particle coherent state reads [45,46]

$$\begin{aligned} |p_1^* p_2^*; \mu_1 \mu_2; \gamma\rangle &= \left(\frac{4m}{q}\right)^{\frac{1}{2}} |p^*\rangle |\theta\phi; \mu_1 \mu_2; \gamma\rangle \\ &= \left(\frac{4m}{q}\right)^{\frac{1}{2}} \sum_{J\lambda} \sqrt{\frac{2J+1}{4\pi}} \\ &\quad \times D_{\lambda, \mu}^J(\phi, \theta, -\phi) |p^*\rangle |J\lambda; \mu_1 \mu_2; \gamma\rangle \end{aligned} \quad (4.1)$$

where $\mu = \mu_1 - \mu_2$ and $q = q(m^2)$, θ, ϕ describe the momentum and the direction of the particle 1 in the center-of-mass system. The summation is over all integral or half-integral values of J . In the two-particle rest frame $\vec{p}^* = 0$ and λ is the component of the spin J along the direction of the z axis. As in the case of single-particle spin states, a boost along the z axis and a rotation define a pure Lorentz transformation Λ_p that brings the state $|p^*\rangle |J\lambda; \mu_1 \mu_2; \gamma\rangle$ from the rest frame to a state with any momentum p on the orbit

$$U(\Lambda_p)(|p^*\rangle |J\lambda; \mu_1 \mu_2; \gamma\rangle) = |p\rangle |J\lambda; \mu_1 \mu_2; \gamma\rangle. \quad (4.2)$$

Here λ is now a helicity of the angular helicity state $|p\rangle |J\lambda; \mu_1 \mu_2; \gamma\rangle$ in the direction of \vec{p} . The states $|p\rangle |J\lambda; \mu_1 \mu_2; \gamma\rangle$ define the irreducible representation of the restricted inhomogeneous Lorentz group. Under any element of the group they transform accordingly

$$U(\Lambda, a)(|p\rangle|J\lambda; \mu_1\mu_2; \gamma\rangle) \\ = \exp(-ip'_\mu a^\mu)|p'\rangle \left(\sum_{\lambda'} D_{\lambda'\lambda}^J(R)|J\lambda'; \mu_1\mu_2; \gamma\rangle \right) \quad (4.3)$$

where $p' = \Lambda p$, $R = \Lambda_p^{-1} \Lambda \Lambda_p$ is a Wigner rotation [45,47] and $D_{\lambda'\lambda}^J(R)$ is the matrix representing the rotation R in the irreducible representation of the rotation group corresponding to spin J .

The intrinsic P -parity of single-particle states is defined in their rest frame. Similarly, the intrinsic P -parity of the angular helicity states is given by a relation in the center-of-mass system [45,46]

$$P(|p^*\rangle|J\lambda; \mu_1\mu_2; \gamma\rangle) \\ = \eta_1\eta_2(-1)^{J-s_1-s_2}|p^*\rangle|J\lambda; -\mu_1-\mu_2; \gamma\rangle \quad (4.4)$$

where η_1, η_2 and s_1, s_2 are the parities and spins of the two particles, respectively. The angular helicity states are parity eigenstates only for two spinless particle states. However, we can write any angular helicity state as a combination of two states with opposite P -parities

$$|J\lambda; \mu_1\mu_2; \gamma\rangle = \frac{1}{2}(|J\lambda+; \mu_1\mu_2; \gamma\rangle + |J\lambda-; \mu_1\mu_2; \gamma\rangle) \quad (4.5)$$

where

$$|J\lambda\pm; \mu_1\mu_2; \gamma\rangle = |J\lambda; \mu_1\mu_2; \gamma\rangle \\ \pm \eta_1\eta_2(-1)^{J-s_1-s_2}|J\lambda; -\mu_1-\mu_2; \gamma\rangle. \quad (4.6)$$

The angular helicity states with a definite P -parity now have a character of single-particle helicity states with variable mass m and quantum numbers γ . We can refer to these states as diparticle spin states. The general two-particle helicity states are a coherent superposition of diparticle spin states

$$|p_1p_2; \mu_1\mu_2; \gamma\rangle = \left(\frac{4m}{q}\right)^{\frac{1}{2}}|p\rangle|\theta\phi; \mu_1\mu_2; \gamma\rangle \\ = \left(\frac{4m}{q}\right)^{\frac{1}{2}} \sum_{J\lambda} \sqrt{\frac{2J+1}{4\pi}} D_{\lambda,\mu}^J(\phi, \theta, -\phi) \\ \times \frac{1}{2}(|p\rangle|J\lambda+; \mu_1\mu_2; \gamma\rangle + |p\rangle|J\lambda-; \mu_1\mu_2; \gamma\rangle). \quad (4.7)$$

For two particles with spin the coherent state $\left(\frac{4m}{q}\right)^{\frac{1}{2}}|p\rangle|\theta\phi; \mu_1\mu_2; \gamma\rangle$ is an angular superposition of diparticle states that form parity doublets. For spinless particles the diparticle states are parity singlets. An extension of this spin formalism for three-particle helicity states was given by Wick [48].

V. AMPLITUDES IN $\pi N \rightarrow \pi\pi N$ PROCESSES

A. Partial wave helicity amplitudes

We consider the pion creation process $\pi_a N_b \rightarrow \pi_1 \pi_2 N_d$ with four-momenta $p_a + p_b = p_1 + p_2 + p_d$. In the laboratory system of the reaction the $+z$ axis has the direction opposite to the incident pion beam. The $+y$ axis is perpendicular to the scattering plane and has a direction of $\vec{p}_a \times \vec{p}_c$ where $p_c = p_1 + p_2$. The angular distribution of the produced dipion system is described by the direction of π_1 in the two-pion center-of-mass system and its solid angle $\Omega = \theta, \phi$. The final state vector for the noninteracting particles is

$$|p_1 0\rangle|p_2 0\rangle|p_d \chi\rangle = \left(\frac{4m}{q}\right)^{\frac{1}{2}}|p_c\rangle|\theta\phi, 00\rangle|p_d \chi\rangle \\ \equiv \left(\frac{4m}{q}\right)^{\frac{1}{2}}|p_c p_d\rangle|\theta\phi, \chi\rangle \quad (5.1)$$

where χ is the recoil nucleon helicity, m is the invariant mass $m^2 = p_c^2$ and $q = q(m^2)$ is the π_1 momentum in the two-pion center-of-mass system. The helicity of the target nucleon is ν . We have seen in Sec. IV that a state vector of two noninteracting particles can be expressed as a coherent superposition of diparticle helicity states with definite spin and parity given by (4.7). For two pions $\mu_1 = \mu_2 = 0$ and $D_{\lambda 0}^J(\phi, \theta, -\phi) = \sqrt{4\pi/(2J+1)}Y_\lambda^{J*}(\theta, \phi)$ [49]. The angular state $|\theta\phi, \chi\rangle$ can be expanded in terms of spherical harmonics

$$|\theta\phi, \chi\rangle = \sum_{J=0}^{\infty} \sum_{\lambda=-J}^J Y_\lambda^{J*}(\theta, \phi)|J\lambda, \chi\rangle. \quad (5.2)$$

The angular expansion of the S -matrix amplitudes $S_{\chi,0\nu}(\theta\phi) = \langle\theta\phi, \chi|\langle p_c p_d|S|p_a p_b, 0\nu\rangle$

$$S_{\chi,0\nu}(\theta\phi) = \sum_{J=0}^{\infty} \sum_{\lambda=-J}^J Y_\lambda^J(\theta, \phi) S_{\lambda\chi,0\nu}^J \quad (5.3)$$

defines partial wave S -matrix amplitudes

$$S_{\lambda\chi,0\nu}^J(p_c p_d, p_a p_b) = \langle J\lambda, \chi|\langle p_c p_d|S|p_a p_b, 0\nu\rangle \quad (5.4)$$

of definite dipion spin. With $S_{\chi,0\nu} = i(2\pi)^4 \delta^4(P_f - P_i) T_{\chi,0\nu}$ the measured helicity amplitudes are defined by

$$H_{\chi,0\nu}(s, t, m, \theta\phi) = \sqrt{q(m^2)G(s)/\text{Flux}(s)} T_{\chi,0\nu}(s, t, m, \theta\phi) \quad (5.5)$$

where s is the center-of-mass energy squared, $t = (p_c - p_a)^2$ is the four-momentum transfer squared, $q(m^2)G(s)$ is the final state Lorentz invariant phase space [12] and

Flux(s) is the incident particle flux. The angular expansion of the production amplitudes (5.5) follows from (5.3)

$$H_{\chi,0\nu}(\theta\phi) = \sum_{J=0}^{\infty} \sum_{\lambda=-J}^J Y_{\lambda}^J(\theta, \phi) H_{\lambda\chi,0\nu}^J \quad (5.6)$$

where $H_{\lambda\chi,0\nu}^J(s, t, m)$ are partial wave helicity amplitudes of definite dipion spin.

B. Constraints from conservation of P -parity

Since pion helicities $\mu_1 = \mu_2 = 0$ the two-pion angular states $|m, \vec{p}_c\rangle \otimes |pJ\lambda; 00\rangle$ have a character of single-particle helicity states for any fixed invariant mass m . The initial and final states in these processes are both separable. The helicity amplitudes $H_{\lambda\chi,0\nu}^J(s, t, m)$ then describe two-body scattering processes $\pi^- + p \rightarrow "J(m^2)" + n$ where " $J(m^2)$ " is the dipion "particle" with spin J and mass m . Describing strong interactions, these amplitudes are expected to conserve P -parity.

P -parity conservation in strong interactions imposes constraints on two-body helicity amplitudes [45,47,50]

$$H_{-\mu_c-\mu_d,-\mu_a-\mu_b} = \eta(-1)^{\mu'-\mu} H_{\mu_c\mu_d,\mu_a\mu_b} \quad (5.7)$$

where $\eta = \eta_a\eta_b\eta_c\eta_d(-1)^{s_c+s_d-s_a-s_b}$ and $\mu = \mu_a - \mu_b$, $\mu' = \mu_c - \mu_d$. The derivation of these constraints requires that the initial and final states are both separable states of single-particle helicity states and that the total angular momentum is conserved in the reaction [45]. These conditions are satisfied by the processes $\pi^- + p \rightarrow "J(m^2)" + n$ and the helicity amplitudes $H_{\lambda\chi,0\nu}^J$ thus must satisfy the parity constraints (5.28). From (4.4) we find that $\eta_{\pi\pi} = (-1)^J$. The parity constraints for $H_{\lambda\chi,0\nu}^J$ then read

$$H_{-\lambda-\chi,0-\nu}^J = (-1)^{\lambda+\chi+\nu} H_{\lambda\chi,0\nu}^J. \quad (5.8)$$

These parity constraints apply to all pion production processes $\pi N \rightarrow \pi\pi N$. The target nucleon and recoil nucleon helicities ν and χ are defined in the s -channel helicity system. The dipion helicity λ will be defined in the t -channel helicity system [6,45,51].

Assuming that all pion isospin states behave as identical particles in strong interactions the generalized Bose-Einstein statistics requires $I + J = \text{even}$ where I is the dipion isospin [45]. As the result, the partial wave helicity amplitudes with odd spins J vanish in reactions with two identical pions in the final state and the $\pi^-\pi^+$ isospin states are maximally entangled symmetric and antisymmetric Bell states for even and odd isospin, respectively.

C. Nucleon helicity and transversity amplitudes with definite t -channel naturality

The helicity amplitudes $H_{\lambda\chi,0\nu}^J$ are combinations of helicity amplitudes with definite t -channel naturality $\eta = \mathcal{P}\mathcal{S}$ where \mathcal{P} and \mathcal{S} are the parity and the signature of Reggeons exchanged in $\pi^- + p \rightarrow "J(m^2)" + n$ [45]. The natural and unnatural exchange amplitudes $N_{\lambda+,0\pm}^J$ and $U_{\lambda+,0\pm}^J$ correspond to naturality $\eta = +1$ and $\eta = -1$, respectively. They are given for $\lambda \neq 0$ by relations [50–52]

$$\begin{aligned} U_{\lambda+,0\pm}^J &= \frac{1}{\sqrt{2}} (H_{\lambda+,0\pm}^J + (-1)^\lambda H_{-\lambda+,0\pm}^J) \\ N_{\lambda+,0\pm}^J &= \frac{1}{\sqrt{2}} (H_{\lambda+,0\pm}^J - (-1)^\lambda H_{-\lambda+,0\pm}^J). \end{aligned} \quad (5.9)$$

For $\lambda = 0$ they are

$$U_{0+,0\pm}^J = H_{0+,0\pm}^J, \quad N_{0+,0\pm}^J = 0. \quad (5.10)$$

In (5.9) and (5.10) $+$ and $-$ correspond to $+\frac{1}{2}$ and $-\frac{1}{2}$ values of nucleon helicities. The unnatural exchange amplitudes $U_{\lambda+,0-}^J$ and $U_{\lambda+,0+}^J$ exchange π and a_1 quantum numbers in the t -channel, respectively, while the natural exchange amplitudes $N_{\lambda+,0-}^J$ and $N_{\lambda+,0+}^J$ both exchange a_2 quantum numbers.

Amplitude analyses of measurements on polarized targets are best performed in terms of transversity amplitudes with definite t -channel naturality [51]. In such measurements the spin states of the target nucleon are described by transversity τ with $\tau = +\frac{1}{2} \equiv u$ and $\tau = -\frac{1}{2} \equiv d$ corresponding to "up" and "down" orientations of the target spin relative to the scattering plane [50,52]. Following Lutz and Rybicki [51], we define mixed helicity-transversity amplitudes with nucleon helicity replaced by nucleon transversity

$$\begin{aligned} T_{\lambda\tau_n,0\tau}^J &= \sum_{\chi,\nu} D_{\tau_n\chi}^{\frac{1}{2}\ast} \left(\frac{\pi}{2}, \frac{\pi}{2}, -\frac{\pi}{2} \right) e^{i\pi(\chi-\nu)} H_{\lambda\chi,0\nu}^J \\ &\quad \times D_{\nu\tau}^{\frac{1}{2}} \left(\frac{\pi}{2}, \frac{\pi}{2}, -\frac{\pi}{2} \right). \end{aligned} \quad (5.11)$$

Using the parity relations (5.8) for helicity amplitudes we obtain

$$\begin{aligned} T_{\lambda u,0u}^J &= \frac{1}{2} (1 - (-1)^\lambda) (H_{\lambda+,0+}^J + iH_{\lambda+,0-}^J) \\ T_{\lambda d,0d}^J &= \frac{1}{2} (1 - (-1)^\lambda) (H_{\lambda+,0+}^J - iH_{\lambda+,0-}^J) \\ -iT_{\lambda d,0u}^J &= \frac{1}{2} (1 + (-1)^\lambda) (H_{\lambda+,0+}^J + iH_{\lambda+,0-}^J) \\ +iT_{\lambda u,0d}^J &= \frac{1}{2} (1 + (-1)^\lambda) (H_{\lambda+,0+}^J - iH_{\lambda+,0-}^J). \end{aligned} \quad (5.12)$$

As a result of parity conservation the following amplitudes vanish

$$\begin{aligned} T_{\lambda\tau,0\tau}^J &= 0 \quad \lambda = \text{even} \\ T_{\lambda-\tau,0\tau}^J &= 0 \quad \lambda = \text{odd}. \end{aligned} \quad (5.13)$$

Absorbing the inessential factors $\pm i$ in front of $T_{\lambda d,0u}^J$ and $T_{\lambda u,0d}^J$ in (5.12) into these amplitudes, the unnatural and natural exchange transversity amplitudes are given for $\lambda = \text{even}$ by

$$\begin{aligned} U_{\lambda,\tau}^J &= \frac{1}{2}(T_{\lambda-\tau,0\tau}^J + (-1)^\lambda T_{-\lambda-\tau,0\tau}^J) \\ N_{\lambda,\tau}^J &= \frac{1}{2}(T_{\lambda-\tau,0\tau}^J - (-1)^\lambda T_{-\lambda-\tau,0\tau}^J) \end{aligned} \quad (5.14)$$

and for $\lambda = \text{odd}$ by

$$\begin{aligned} U_{\lambda,\tau}^J &= \frac{1}{2}(T_{\lambda\tau,0\tau}^J + (-1)^\lambda T_{-\lambda\tau,0\tau}^J) \\ N_{\lambda,\tau}^J &= \frac{1}{2}(T_{\lambda\tau,0\tau}^J - (-1)^\lambda T_{-\lambda\tau,0\tau}^J). \end{aligned} \quad (5.15)$$

For $\lambda = \text{even}$ the recoil nucleon transversity $\tau_n = -\tau$. For $\lambda = \text{odd}$, $\tau_n = +\tau$. Note that $N_{0,\tau}^J = 0$. From (5.14) and (5.15) we find parity relations

$$U_{-\lambda,\tau}^J = +(-1)^\lambda U_{\lambda,\tau}^J, \quad N_{-\lambda,\tau}^J = -(-1)^\lambda N_{\lambda,\tau}^J. \quad (5.16)$$

It is useful to express transversity amplitudes $U_{\lambda,\tau}^J$ and $N_{\lambda,\tau}^J$ in terms of unnatural and natural exchange helicity amplitudes (5.9). Using (5.12) and (5.9) in (5.14) and (5.15) we find

$$\begin{aligned} U_{\lambda,u}^J &= \frac{1}{\sqrt{2}}(U_{\lambda+,0+}^J + iU_{\lambda+,0-}^J) \\ U_{\lambda,d}^J &= \frac{1}{\sqrt{2}}(U_{\lambda+,0+}^J - iU_{\lambda+,0-}^J) \end{aligned} \quad (5.17)$$

$$\begin{aligned} N_{\lambda,u}^J &= \frac{1}{\sqrt{2}}(N_{\lambda+,0+}^J + iN_{\lambda+,0-}^J) \\ N_{\lambda,d}^J &= \frac{1}{\sqrt{2}}(N_{\lambda+,0+}^J - iN_{\lambda+,0-}^J). \end{aligned} \quad (5.18)$$

VI. FINAL STATE DENSITY MATRIX IN $\pi N \rightarrow \pi\pi N$ PROCESSES

A. Angular final state density matrix

The pion beam and nucleon target are prepared in an initial state $\rho_i = \rho_i(\pi_a) \otimes \rho_i(N_b, \vec{P})$ where $\rho_i(\pi_a) = |p_a 0\rangle\langle p_a 0|$ and

$$\rho_i(N_b, \vec{P}) = \sum_{\nu\nu'} \rho_b(\vec{P})_{\nu\nu'} |p_b \nu\rangle\langle p_b \nu'|. \quad (6.1)$$

$\rho_b(\vec{P})$ is the target nucleon spin density matrix

$$\rho_b(\vec{P}) = \frac{1}{2}(1 + \vec{P} \vec{\sigma}) \quad (6.2)$$

where $\vec{P} = (P_x, P_y, P_z)$ is the target polarization vector, $\vec{\sigma} = (\sigma_x, \sigma_y, \sigma_z)$ are Pauli matrices and $\text{Tr}(\rho_b(\vec{P})) = 1$. Following (3.5) the density matrix $\rho_f(\vec{P})$ of the final state $\pi_1 \pi_2 N_d$ reads

$$\begin{aligned} \rho_f(\vec{P}) &= \sum_{\chi\chi'} \int d\Phi_3 d\Phi_3' \langle \theta\phi, \chi, p_c p_d | S \rho_i S^\dagger | p'_c p'_d, \theta'\phi', \chi' \rangle \\ &\quad \times |p_c p_d, \theta\phi, \chi\rangle \langle \theta'\phi', \chi', p'_c p'_d| \end{aligned} \quad (6.3)$$

where we have used the phase space relation [45]

$$d\Phi_3 = \frac{d^3 \vec{p}_1}{2E_1} \frac{d^3 \vec{p}_2}{2E_2} \frac{d^3 \vec{p}_3}{2E_3} = \frac{q}{4m} d^4 p_c d\Omega \frac{d^3 \vec{p}_3}{2E_3} = d\bar{\Phi}_3 d\Omega \quad (6.4)$$

in the completeness relation (3.2). We shall use the projection of $\rho_f(\vec{P})$ into an angular state $\rho_f(p_c p_d, \theta\phi, \vec{P})$ with definite final state momenta

$$\rho_f(p_c p_d, \theta\phi, \vec{P}) = \sum_{\chi\chi'} \rho_f(p_c p_d, \theta\phi, \vec{P})_{\chi\chi'} |\chi\rangle\langle\chi'|. \quad (6.5)$$

In the following we suppress the momentum labels in the initial and final helicity states. The density matrix elements are given by the S -matrix evolution law

$$\rho_f(\theta\phi, \vec{P})_{\chi\chi'} = \sum_{\nu\nu'} \langle \theta\phi, \chi | S | 0\nu \rangle \rho_b(\vec{P})_{\nu\nu'} \langle 0\nu' | S^\dagger | \theta\phi, \chi' \rangle. \quad (6.6)$$

With $S_{\chi,0\nu} = \langle \theta\phi, \chi | S | 0\nu \rangle = i(2\pi)^4 \delta^4(P_f - P_i) T_{\chi,0\nu}$ we get

$$\rho_f(\theta\phi, \vec{P})_{\chi\chi'} = \rho_f'(\theta\phi, \vec{P})_{\chi\chi'} (VT) (2\pi)^4 \delta^4(P_f - P_i) \quad (6.7)$$

where $\rho_f'(\theta\phi, \vec{P})$ is expressed in terms of transition amplitudes $T_{\chi,0\nu}$ and where we have used the conventional approach to deal with a square of δ -functions [47] with V and T being total volume and time confining the interactions to be taken in the limit $V, T \rightarrow \infty$. According to the Born rule, the probability of $\pi_a N_b(\nu) \rightarrow \pi_1 \pi_2 N_d(\chi)$ is given by

$$dP_{\chi,0\nu} = |S_{\chi,0\nu}|^2 \prod_{n=1}^d \frac{d^3 \vec{p}_n}{2E_n} \\ = |T_{\chi,0\nu}|^2 d\text{Lips}(P_i, p_1, p_2, p_d)(VT). \quad (6.8)$$

Here $P_i = p_a + p_b$ is the total four-momentum and the Lorentz invariant phase space $d\text{Lips} = q(m^2)G(s)dmdtd\Omega$ where $G(s)$ is the energy dependent part of the phase space [12]. The probability per unit volume, unit time and per target particle is $d\sigma_{\chi,0\nu} = dP_{\chi,0\nu}/(VT\text{Flux}(s))$ and the differential cross section reads

$$\frac{d\sigma_{\chi,0\nu}}{dtdmd\Omega} = \frac{q(m^2)G(s)}{\text{Flux}(s)} |T_{\chi,0\nu}|^2. \quad (6.9)$$

Applying formally the same procedure to every bilinear term $S_{\chi,0\nu} S_{\chi',0\nu}^*$ of $\rho_f(\theta\phi, \vec{P})$ we can define a differential cross-section matrix

$$\frac{d\sigma}{dtdmd\Omega} = \frac{q(m^2)G(s)}{\text{Flux}(s)} \rho_f'(\theta\phi, \vec{P}) \equiv \rho_f(\theta\phi, \vec{P}) \quad (6.10)$$

where we have redefined the final state density matrix $\rho_f(\theta\phi, \vec{P})$ to read

$$\rho_f(\theta\phi, \vec{P})_{\chi\chi'} = \sum_{\nu\nu'} H_{\chi,0\nu}(\theta\phi) \rho_b(\vec{P})_{\nu\nu'} H_{\chi',0\nu'}^*(\theta\phi). \quad (6.11)$$

Introducing the recoil nucleon polarization vector $\vec{Q}(\theta\phi, \vec{P})$ using a relation [50,52]

$$\vec{I}(\theta\phi, \vec{P}) \equiv \vec{Q}(\theta\phi, \vec{P}) I^0(\theta\phi, \vec{P}) \quad (6.15)$$

we can write

$$\rho_f(\theta\phi, \vec{P}) = \frac{1}{2} (1 + \vec{Q}(\theta\phi, \vec{P}) \vec{\sigma}) I^0(\theta\phi, \vec{P}) \\ = \rho_d(\vec{Q}) I^0(\theta\phi, \vec{P}) \quad (6.16)$$

where $\rho_d(\vec{Q}) = \frac{1}{2} (1 + \vec{Q} \vec{\sigma})$ is the recoil nucleon spin density matrix. The polarization vector $\vec{Q} = (Q^1, Q^2, Q^3)$ is defined in the rest frame of the recoil nucleon. It has a transverse component Q^2 that is perpendicular to the scattering plane in the direction of the y axis. The transverse

The redefined transition amplitudes $H_{\chi,0\nu}(s, t, m, \theta\phi)$ are given by (5.5) in Sec. V.

B. Recoil nucleon polarization

To discuss the structure of the angular final state density matrix (6.12) we first note a useful result from quantum state tomography [3]. An arbitrary density matrix ρ of n qubits can be expanded in a form

$$\rho = \sum_{\vec{v}} \left(\frac{1}{2^n} \right) \text{Tr}(\sigma_{v_1} \otimes \sigma_{v_2} \otimes \cdots \otimes \sigma_{v_n} \rho) \sigma_{v_1} \\ \otimes \sigma_{v_2} \otimes \cdots \otimes \sigma_{v_n} \quad (6.12)$$

where the sum is over the vectors $\vec{v} = (v_1, v_2, \dots, v_n)$ with entries chosen from the set $\sigma^j, j = 0, 1, 2, 3$ of Pauli matrices and $\sigma^0 = \mathbb{1}$. The traces in (6.12) represent average values of spin correlations. The final density matrix $\rho_f(\theta\phi, \vec{P})$ is a single qubit density matrix corresponding to spin $\frac{1}{2}$ of the recoil nucleon. It can be written in the form (6.12)

$$\rho_f(\theta\phi, \vec{P}) = \frac{1}{2} (I^0(\theta\phi, \vec{P}) \sigma^0 + \vec{I}(\theta\phi, \vec{P}) \vec{\sigma}) \quad (6.13)$$

where the traces $I^j(\theta\phi, \vec{P}) = \text{Tr}(\sigma^j \rho_f(\theta\phi, \vec{P}))$, $j = 0, 1, 2, 3$ represent measurable intensities of angular distributions. The density matrix can be written in an equivalent form in the recoil nucleon helicity basis $|\chi\rangle\langle\chi'|$

$$\rho_f(\theta\phi, \vec{P}) = \begin{pmatrix} I^0(\theta\phi, \vec{P}) + I^3(\theta\phi, \vec{P}), & I^1(\theta\phi, \vec{P}) - iI^2(\theta\phi, \vec{P}) \\ I^1(\theta\phi, \vec{P}) + iI^2(\theta\phi, \vec{P}), & I^0(\theta\phi, \vec{P}) - I^3(\theta\phi, \vec{P}) \end{pmatrix}. \quad (6.14)$$

component Q^1 is perpendicular to the direction of the recoil nucleon in the scattering plane. The longitudinal component Q^3 is along the direction of its motion.

Equation (6.16) is our principal result. It shows that the purity of the final state $\rho_f(\theta\phi, P)$ is controlled entirely by the recoil nucleon polarization $\vec{Q}(\theta\phi, \vec{P})$ which we shall relate in the following to partial wave transversity amplitudes under the assumption of P -parity conservation.

C. Angular intensities in terms of density matrix elements

To measure the final state density matrix (6.13) requires measurements of angular intensities the measurement of which is further reduced to the measurements of density matrix elements in terms of amplitudes. Using the target nucleon spin density matrix (6.2) in the expression (6.11) we can write the matrix elements of $\rho_f(\theta\phi, \vec{P})$ in terms of components of target polarization

$$\begin{aligned} \rho_f(\theta\phi, \vec{P})_{\chi\chi'} &= \rho_u(\theta\phi)_{\chi\chi'} + P_x \rho_x(\theta\phi)_{\chi\chi'} \\ &+ P_y \rho_y(\theta\phi)_{\chi\chi'} + P_z \rho_z(\theta\phi)_{\chi\chi'} \end{aligned} \quad (6.17)$$

where the subscript u stands for the unpolarized target $\vec{P} = 0$. The polarization components of density matrix elements in (6.17) are given by (6.11)

$$\rho_k(\theta\phi)_{\chi\chi'} = \frac{1}{2} \sum_{\nu\nu'} H_{\chi,0\nu}(\theta\phi)(\sigma_k)_{\nu\nu'} H_{\chi',0\nu'}^*(\theta\phi) \quad (6.18)$$

where $k = u, x, y, z$ and $\sigma_u \equiv \sigma_0$. Using (5.6) for $H_{\chi,0\nu}(\theta\phi)$ their angular expansion reads

$$\rho_k(\theta\phi)_{\chi\chi'} = \sum_{J\lambda} \sum_{J'\lambda'} (R_k)^{J\lambda, J'\lambda'} Y_\lambda^J(\theta, \phi) Y_{\lambda'}^{J'*}(\theta, \phi) \quad (6.19)$$

where

$$(R_k)^{J\lambda, J'\lambda'} = \frac{1}{2} \sum_{\nu\nu'} H_{\chi,0\nu}^J(\sigma_k)_{\nu\nu'} H_{\chi',0\nu'}^{J'*}. \quad (6.20)$$

Using the decomposition (6.17) for $\rho_f(\theta\phi, \vec{P})$ we find a decomposition for the intensities $I^j(\theta\phi, \vec{P})$ in (6.13) in terms of components of the target polarization

$$\begin{aligned} I^j(\theta\phi, \vec{P}) &= \text{Tr}(\sigma^j \rho_f(\theta\phi, \vec{P})) \\ &= I_u^j(\theta\phi) + P_x I_x^j(\theta\phi) + P_y I_y^j(\theta\phi) + P_z I_z^j(\theta\phi) \end{aligned} \quad (6.21)$$

where the components $I_k^j(\theta\phi)$, $j = 0, 1, 2, 3$ and $k = u, x, y, z$ are given by traces

$$I_k^j(\theta\phi) = \text{Tr}_{\chi\chi'}((\sigma^j)_{\chi\chi'} \rho_k(\theta\phi)_{\chi\chi'}). \quad (6.22)$$

The component intensities $I_k^j(\theta\phi)$ have angular expansions arising from these traces

$$I_k^j(\theta\phi) = \sum_{J\lambda} \sum_{J'\lambda'} (R_k^j)^{J\lambda, J'\lambda'} Y_\lambda^J(\theta, \phi) Y_{\lambda'}^{J'*}(\theta, \phi) \quad (6.23)$$

where the un-normalized dipion density matrix elements $(R_k^j)^{J\lambda, J'\lambda'}$ are traces over recoil nucleon helicities

$$(R_k^j)^{J\lambda, J'\lambda'} = \text{Tr}_{\chi\chi'}((\sigma^j)_{\chi\chi'} (R_k)^{J\lambda, J'\lambda'}). \quad (6.24)$$

Expressed in terms of partial wave helicity amplitudes they read

$$(R_k^j)^{J\lambda, J'\lambda'} = \frac{1}{2} \sum_{\chi\chi'} \sum_{\nu\nu'} (\sigma^j)_{\chi\chi'} H_{\chi,0\nu}^J(\sigma_k)_{\nu\nu'} H_{\chi',0\nu'}^{J'*}. \quad (6.25)$$

Combining (6.19) and (6.23) in (6.14) we can express the density matrix elements (6.20) in terms of density matrix elements (6.25) for each $k = u, x, y, z$

$$\begin{aligned} (R_k)^{J\lambda, J'\lambda'} &= (R_k^0)^{J\lambda, J'\lambda'} + (R_k^3)^{J\lambda, J'\lambda'} \\ (R_k)^{J\lambda, J'\lambda'} &= (R_k^1)^{J\lambda, J'\lambda'} - i(R_k^2)^{J\lambda, J'\lambda'} \\ (R_k)^{J\lambda, J'\lambda'} &= (R_k^1)^{J\lambda, J'\lambda'} + i(R_k^2)^{J\lambda, J'\lambda'} \\ (R_k)^{J\lambda, J'\lambda'} &= (R_k^0)^{J\lambda, J'\lambda'} - (R_k^3)^{J\lambda, J'\lambda'}. \end{aligned} \quad (6.26)$$

D. Constraints on angular intensities from P -parity conservation

Conservation of P -parity in strong interactions is encoded in the angular expansion of the angular final state density matrix by imposing parity relations on the partial wave helicity amplitudes. Relabeling the summations in (6.23) and combining in the sum (6.23) the terms with inverted $J\lambda$ and $J'\lambda'$ we can write the sum (6.23) for each $k = u, y, x, y$ and $j = 0, 1, 2, 3$ as the sum of four terms

$$\begin{aligned} \frac{1}{4} \sum_{J\lambda} \sum_{J'\lambda'} [R_{\lambda\lambda'}^{JJ'} Y_\lambda^J Y_{\lambda'}^{J'*} + R_{\lambda'\lambda}^{J'J} Y_{\lambda'}^{J'} Y_\lambda^{J*} \\ + R_{-\lambda-\lambda'}^{JJ'} Y_{-\lambda}^J Y_{-\lambda'}^{J'*} + R_{-\lambda'-\lambda}^{J'J} Y_{-\lambda'}^{J'} Y_{-\lambda}^{J*}]. \end{aligned} \quad (6.27)$$

Using the Hermiticity of the density matrix

$$(R_k^j)^{J\lambda, J'\lambda'} = (R_k^j)^{J'\lambda', J\lambda} \quad (6.28)$$

and a relation for spherical harmonics $Y_{-M}^L(\theta, \phi) = (-1)^M (Y_M^L(\theta, \phi))^*$ the sum of terms in (6.27) takes the form

$$\begin{aligned} [+2\text{Re}(R_{\lambda\lambda'}^{JJ'} + (-1)^{\lambda+\lambda'} R_{-\lambda-\lambda'}^{JJ'*}) \text{Re}(Y_\lambda^J Y_{\lambda'}^{J'*}) \\ - 2\text{Im}(R_{\lambda\lambda'}^{JJ'} - (-1)^{\lambda+\lambda'} R_{-\lambda-\lambda'}^{JJ'*}) \text{Im}(Y_\lambda^J Y_{\lambda'}^{J'*})]. \end{aligned} \quad (6.29)$$

Parity relations (5.8) for the partial wave helicity amplitudes $H_{\chi,0\nu}^J$ imply parity relations for the density matrix elements

$$(R_k^j)^{J\lambda, J'\lambda'} = +(-1)^{\lambda+\lambda'} (R_k^j)^{J'\lambda', J\lambda} \quad (6.30)$$

for $(k, j) = (u, 0), (y, 0), (u, 2), (y, 2), (x, 1), (z, 1), (x, 3), (z, 3)$ and

$$(R_k^j)^{J\lambda, J'\lambda'} = -(-1)^{\lambda+\lambda'} (R_k^j)^{J'\lambda', J\lambda} \quad (6.31)$$

for $(x, 0), (z, 0), (x, 2), (z, 2), (u, 1), (y, 1), (u, 3), (y, 3)$. Using these symmetry relations in (6.29) the components $I_k^j(\theta\phi)$ of the dipion angular distribution $I^j(\theta\phi, \vec{P})$ measured on polarized target take the form

$$I_k^j(\theta\phi) = \sum_{J\lambda} \sum_{J'\lambda'} (\text{Re}R_k^{JJ'} \text{Re}(Y_\lambda^j(\theta\phi) Y_{\lambda'}^{j'*}(\theta\phi))) \quad (6.32)$$

for $(k, j) = (u, 0), (y, 0), (u, 2), (y, 2), (x, 1), (z, 1), (x, 3), (z, 3)$ and

$$I_k^j(\theta\phi) = -\sum_{J\lambda} \sum_{J'\lambda'} (\text{Im}R_k^{JJ'} \text{Im}(Y_\lambda^j(\theta\phi) Y_{\lambda'}^{j'*}(\theta\phi))) \quad (6.33)$$

for $(x, 0), (z, 0), (x, 2), (z, 2), (u, 1), (y, 1), (u, 3), (y, 3)$. The elements $(\text{Im}R_k^{JJ'})$ in the group (6.32) and $(\text{Re}R_k^{JJ'})$ in the group (6.33) are not observable as the result of parity conservation.

Because of the angular properties of $Y_\lambda^j(\theta\phi)$, the three elements $(R_k^j)_{00}^{00}$, $(R_k^j)_{00}^{11}$ and $(R_k^j)_{11}^{11}$ in (6.32) are not independent in $\pi^- p \rightarrow \pi^- \pi^+ n$ but appear in two independent combinations

$$\begin{aligned} (R_k^j)_{SP} &\equiv (R_k^j)_{00}^{00} + (R_k^j)_{00}^{11} + 2(R_k^j)_{11}^{11}, \\ (R_k^j)_{PP} &\equiv (R_k^j)_{00}^{11} - (R_k^j)_{11}^{11}. \end{aligned} \quad (6.34)$$

What are usually measured in actual experiments are normalized density matrix elements $(\rho_k^j)_{\lambda\lambda'}$ defined by

$$(R_k^j)_{\lambda\lambda'}^{JJ'} = \frac{d^2\sigma}{dt dm} (\rho_k^j)_{\lambda\lambda'}^{JJ'} \quad (6.35)$$

where

TABLE I. Density matrix elements expressed in terms of nucleon transversity amplitudes with definite t -channel naturality. The spin indices JJ' which always go with helicities $\lambda\lambda'$ have been omitted in the amplitudes. The coefficients $\eta_\lambda = 1$ for $\lambda = 0$ and $\eta_\lambda = 1/\sqrt{2}$ for $\lambda \neq 0$.

$(R_u^0)_{\lambda\lambda'}^{JJ'}$	$\eta_\lambda \eta_{\lambda'} [U_{\lambda,u} U_{\lambda',u}^* + N_{\lambda,u} N_{\lambda',u}^* + U_{\lambda,d} U_{\lambda',d}^* + N_{\lambda,d} N_{\lambda',d}^*]$
$(R_y^0)_{\lambda\lambda'}^{JJ'}$	$\eta_\lambda \eta_{\lambda'} [U_{\lambda,u} U_{\lambda',u}^* + N_{\lambda,u} N_{\lambda',u}^* - U_{\lambda,d} U_{\lambda',d}^* - N_{\lambda,d} N_{\lambda',d}^*]$
$(R_x^0)_{\lambda\lambda'}^{JJ'}$	$-i\eta_\lambda \eta_{\lambda'} [U_{\lambda,u} N_{\lambda',d}^* + N_{\lambda,u} U_{\lambda',d}^* - U_{\lambda,d} N_{\lambda',u}^* - N_{\lambda,d} U_{\lambda',u}^*]$
$(R_z^0)_{\lambda\lambda'}^{JJ'}$	$\eta_\lambda \eta_{\lambda'} [U_{\lambda,u} N_{\lambda',d}^* + N_{\lambda,u} U_{\lambda',d}^* + U_{\lambda,d} N_{\lambda',u}^* + N_{\lambda,d} U_{\lambda',u}^*]$
$(R_u^2)_{\lambda\lambda'}^{JJ'}$	$-\eta_\lambda \eta_{\lambda'} [U_{\lambda,u} U_{\lambda',u}^* - N_{\lambda,u} N_{\lambda',u}^* - U_{\lambda,d} U_{\lambda',d}^* + N_{\lambda,d} N_{\lambda',d}^*]$
$(R_y^2)_{\lambda\lambda'}^{JJ'}$	$-\eta_\lambda \eta_{\lambda'} [U_{\lambda,u} U_{\lambda',u}^* - N_{\lambda,u} N_{\lambda',u}^* + U_{\lambda,d} U_{\lambda',d}^* - N_{\lambda,d} N_{\lambda',d}^*]$
$(R_x^2)_{\lambda\lambda'}^{JJ'}$	$i\eta_\lambda \eta_{\lambda'} [U_{\lambda,u} N_{\lambda',d}^* - N_{\lambda,u} U_{\lambda',d}^* + U_{\lambda,d} N_{\lambda',u}^* - N_{\lambda,d} U_{\lambda',u}^*]$
$(R_z^2)_{\lambda\lambda'}^{JJ'}$	$-\eta_\lambda \eta_{\lambda'} [U_{\lambda,u} N_{\lambda',d}^* - N_{\lambda,u} U_{\lambda',d}^* - U_{\lambda,d} N_{\lambda',u}^* + N_{\lambda,d} U_{\lambda',u}^*]$
$(R_u^1)_{\lambda\lambda'}^{JJ'}$	$-i\eta_\lambda \eta_{\lambda'} [U_{\lambda,u} N_{\lambda',u}^* - N_{\lambda,u} U_{\lambda',u}^* - U_{\lambda,d} N_{\lambda',d}^* + N_{\lambda,d} U_{\lambda',d}^*]$
$(R_y^1)_{\lambda\lambda'}^{JJ'}$	$-i\eta_\lambda \eta_{\lambda'} [U_{\lambda,u} N_{\lambda',u}^* - N_{\lambda,u} U_{\lambda',u}^* + U_{\lambda,d} N_{\lambda',d}^* - N_{\lambda,d} U_{\lambda',d}^*]$
$(R_x^1)_{\lambda\lambda'}^{JJ'}$	$-\eta_\lambda \eta_{\lambda'} [U_{\lambda,u} U_{\lambda',d}^* - N_{\lambda,u} N_{\lambda',d}^* + U_{\lambda,d} U_{\lambda',u}^* - N_{\lambda,d} N_{\lambda',u}^*]$
$(R_z^1)_{\lambda\lambda'}^{JJ'}$	$-i\eta_\lambda \eta_{\lambda'} [U_{\lambda,u} U_{\lambda',d}^* - N_{\lambda,u} N_{\lambda',d}^* - U_{\lambda,d} U_{\lambda',u}^* + N_{\lambda,d} N_{\lambda',u}^*]$
$(R_u^3)_{\lambda\lambda'}^{JJ'}$	$\eta_\lambda \eta_{\lambda'} [U_{\lambda,u} N_{\lambda',u}^* + N_{\lambda,u} U_{\lambda',u}^* + U_{\lambda,d} N_{\lambda',d}^* + N_{\lambda,d} U_{\lambda',d}^*]$
$(R_y^3)_{\lambda\lambda'}^{JJ'}$	$\eta_\lambda \eta_{\lambda'} [U_{\lambda,u} N_{\lambda',u}^* + N_{\lambda,u} U_{\lambda',u}^* - U_{\lambda,d} N_{\lambda',d}^* - N_{\lambda,d} U_{\lambda',d}^*]$
$(R_x^3)_{\lambda\lambda'}^{JJ'}$	$-i\eta_\lambda \eta_{\lambda'} [U_{\lambda,u} U_{\lambda',d}^* + N_{\lambda,u} N_{\lambda',d}^* - U_{\lambda,d} U_{\lambda',u}^* - N_{\lambda,d} N_{\lambda',u}^*]$
$(R_z^3)_{\lambda\lambda'}^{JJ'}$	$\eta_\lambda \eta_{\lambda'} [U_{\lambda,u} U_{\lambda',d}^* + N_{\lambda,u} N_{\lambda',d}^* + U_{\lambda,d} U_{\lambda',u}^* + N_{\lambda,d} N_{\lambda',u}^*]$

$$\frac{d^2\sigma}{dt dm} \equiv \int d\Omega I_u^0(\theta\phi) = \sum_{J\lambda} (R_u^0)_{\lambda\lambda}^{JJ} = \frac{1}{2} \sum_{J\lambda} \sum_{\chi,\nu} |H_{\lambda\chi,0\nu}^J|^2 \quad (6.36)$$

is the integrated intensity of $\pi\pi$ production measured on an unpolarized target.

We have expressed the density matrix elements $(R_k^j)_{\lambda\lambda'}^{JJ'}$ in terms of transversity amplitudes $U_{\lambda,\tau}^J$ and $N_{\lambda,\tau}^J$. The results are given in Table I and agree with Ref. [51]. The normalization of the amplitudes is given by the trace (6.36)

$$\frac{d^2\sigma}{dt dm} = \sum_{J,\lambda \geq 0} \sum_{\tau} |U_{\lambda,\tau}^J|^2 + |N_{\lambda,\tau}^J|^2. \quad (6.37)$$

VII. UNITARY EVOLUTION CONSTRAINTS IN $\pi N \rightarrow \pi\pi N$ PROCESSES

A. Constraints on angular intensities

The initial πN state is in a pure state only when the target nucleon is in a pure spin state. The target nucleon spin density matrix has the form $\rho_b(\vec{P}) = \frac{1}{2}(1 + \vec{P}\vec{\sigma})$ where $\vec{P} = (P_x, P_y, P_z)$ is the target polarization vector. The target is in a pure state if and only if $|\vec{P}|^2 = 1$ [3] or, equivalently, $\det(\rho_b(\vec{P})) = 1 - P_x^2 - P_y^2 - P_z^2 = 0$. This condition can be written in the form

$$\sum_{m,n=u}^z \eta_{mn} P_m P_n = 0 \quad (7.1)$$

where $P_u = 1$ and $\eta_{mn} = \text{diag}(+1, -1, -1, -1)$ is the Minkowski metric. In modern polarized targets the density matrix $\rho_b(\vec{P})$ is a mixed state with $|\vec{P}|^2 < 1$ that can be varied by using external magnetic fields to rotate the polarization vector \vec{P} into any desired direction [50]. For $\vec{P} = 0$ the target is unpolarized. The pure states define a Bloch sphere within which are located the mixed states.

As shown in (6.16), the normalized final state density matrix is equal to the recoil nucleon spin density matrix $\rho_d(\vec{Q}) = \frac{1}{2}(1 + \vec{Q}\vec{\sigma})$. The final $\pi\pi N$ state is therefore in a pure state if and only if $|\vec{Q}|^2 = 1$ or, in terms of the intensities (6.15), if and only if $(I^0)^2 - (I^1)^2 - (I^2)^2 - (I^3)^2 = 0$. Using the decomposition (6.21) this last condition takes the form

$$\sum_{m,n=u}^z A_{mn} P_m P_n = 0 \quad (7.2)$$

where

$$A_{mn} = \sum_{j=1}^3 I_m^j I_n^j - I_m^0 I_n^0. \quad (7.3)$$

The purity condition (7.2) must hold true for all polarization vectors \vec{P} which satisfy the purity condition (7.1) and for all values of the kinematic variables s, t, m, θ, ϕ . The intensities I_k^j do not depend on the components P_m of the polarization vector because the S -matrix amplitudes do not depend on the target polarization vector. With all terms A_{mn} independent of the polarization vector, the condition (7.2) is not an independent quadratic form in $P_m P_n$ on the entire Bloch sphere but must coincide with the condition (7.1). That happens if and only if $A_{mn} = \eta_{mn} Z(s, t, m, \theta, \phi)$ which implies that $Z = A_{uu}$. Unitary evolution then imposes 9 independent constraints

$$A_{mn} = \eta_{mn} A_{uu}. \quad (7.4)$$

Explicitly, the unitary evolution constraints on angular intensities read

$$\sum_{j=1}^3 (I_u^j)^2 + (I_k^j)^2 = (I_u^0)^2 + (I_k^0)^2 \quad (7.5)$$

for $A_{kk} = -A_{uu}$, $k = x, y, z$,

$$\sum_{j=1}^3 I_u^j I_k^j = I_u^0 I_k^0 \quad (7.6)$$

for $A_{uk} = 0$, $k = x, y, z$ and

$$\sum_{j=1}^3 I_m^j I_n^j = I_m^0 I_n^0 \quad (7.7)$$

for $A_{mn} = 0$, $m, n = x, y, z$ and $m \neq n$. The three constraints (7.5) are equivalent to three constraints

$$\sum_{j=1}^3 (I_m^j)^2 - (I_n^j)^2 = (I_m^0)^2 - (I_n^0)^2 \quad (7.8)$$

for $A_{mm} - A_{nn} = 0$, $m, n = x, y, z$ and $m \neq n$. The constraints (7.5) and (7.6) can be combined to read

$$\sum_{j=1}^3 (I_u^j \pm I_k^j)^2 = (I_u^0 \pm I_k^0)^2 \quad (7.9)$$

for $k = x, y, z$. These last constraints (7.9) are identical to conditions $|\vec{Q}|^2 = 1$ for special pure initial states with polarizations $P_k = \pm 1$.

Mixed target spin states evolve into mixed recoil nucleon spin states. The conditions (7.1) and (7.2) change to read

$$\sum_{m,n=u}^z \eta_{mn} P_m P_n > 0 \quad (7.10)$$

$$\sum_{m,n=u}^z A_{mn} P_m P_n > 0 \quad (7.11)$$

implying the same constraints (7.4) as in the case of the pure states. The conditions (7.11) also exclude the possibility that $A_{mn} = 0$ for all m, n which is allowed by (7.2).

B. Constraints on parity conserving nucleon transversity amplitudes

We looked for constraints on parity conserving transversity amplitudes implied by the unitarity constraints (7.2) on angular intensities using the expressions for $(R_k^j)_{\lambda\lambda'}^{JJ'}$ given in Table I and the parity relations (6.30) and (6.31) in the angular expansions of the intensities (6.32) and (6.33). We found that the combined constraints (7.9) for $k = y$ corresponding to $A_{yy} = -A_{uu}$ and $A_{uy} = 0$ and the constraints $A_{xz} = 0$ and $A_{xx} = A_{zz}$ are unconditional identities. In the Appendix we show that the constraint $A_{xx} = -A_{uu}$ holds true if and only if at least one of the following two constraints on the transversity amplitudes holds true

$$\begin{aligned} \sum_{J,\lambda \geq 0} \sum_{K,\mu > 0} \eta_\lambda \eta_\mu \xi_\lambda \xi_\mu \text{Im}(U_{\lambda u}^J N_{\mu d}^{K*}) \text{Re} Y_\lambda^J(\Omega) \text{Im} Y_\mu^K(\Omega) = 0 \\ \sum_{J',\lambda' \geq 0} \sum_{K',\mu' > 0} \eta_{\lambda'} \eta_{\mu'} \xi_{\lambda'} \xi_{\mu'} \text{Im}(U_{\lambda' d}^{J'} N_{\mu' u}^{K'}) \text{Re} Y_{\lambda'}^{J'}(\Omega) \text{Im} Y_{\mu'}^{K'}(\Omega) = 0 \end{aligned} \quad (7.12)$$

for all $\Omega = \theta, \phi$ and all s, t, m . The constraints $A_{ux} = 0, A_{uz} = 0, A_{xy} = 0, A_{yz} = 0$ are identities provided that both these constraints hold true. In (7.12) $\eta_\lambda = 1, \xi_\lambda = 1$ for $\lambda = 0$ and $\eta_\lambda = \frac{1}{\sqrt{2}}, \xi_\lambda = 2$ for $\lambda > 0$.

The constraints (7.12) imply constraints on the transversity amplitudes

$$\text{Im}(U_{\lambda\tau}^J N_{\mu-\tau}^{K*}) = 0 \quad (7.13)$$

that must hold true for all values of J, λ, K, μ, τ at all values of kinematic variables s, t, m . To prove (7.13) we recall that at any dipion mass there is a finite number of contributing partial waves with $J \leq J_{\max}(m)$ so that the sums (7.12) are truncated. Let N be the number of the contributing terms. We can select N different values of $\Omega_i, i = 1, N$ transforming (7.12) into a pair of N linear homogeneous equations for the unknown N terms given by the lhs of (7.13). We can select the values of Ω_i such that the determinant of each system is nonzero which ensures that the unknown terms $(\text{Im}(U_{\lambda\tau}^J N_{\mu-\tau}^{K*}))_i, i = 1, N$ must all vanish.

C. Unitary phases and their self-consistency

For amplitudes with nonvanishing moduli the conditions (7.13) imply unitary relative phases between the amplitudes $U_{\lambda\tau}^J N_{\mu-\tau}^{K*}$

$$\Phi(U_{\lambda\tau}^J) - \Phi(N_{\mu-\tau}^{K*}) = 0, \pm\pi, \pm 2\pi. \quad (7.14)$$

Keeping $N_{\mu-\tau}^{K*}$ or $U_{\lambda\tau}^J$ fixed, this condition implies unitary relative phases also between amplitudes $U_{\lambda\tau}^J U_{\lambda'\tau}^{J'*}$ and $N_{\mu\tau}^K N_{\mu'\tau}^{K'*}$

$$\begin{aligned} \Phi(U_{\lambda\tau}^J) - \Phi(U_{\lambda'\tau}^{J'*}) &= 0, \pm\pi, \pm 2\pi \\ \Phi(N_{\mu\tau}^K) - \Phi(N_{\mu'\tau}^{K'*}) &= 0, \pm\pi, \pm 2\pi. \end{aligned} \quad (7.15)$$

We shall refer to such S -matrix amplitudes as unitary amplitudes. It follows from (7.14) and Table I that all elements $R_z^0 = R_z^2 = 0$ so that the intensities $I_z^0 = I_z^2 = 0$.

The relative phases of all S -matrix amplitudes must satisfy a phase condition

$$\Phi(A) - \Phi(B) = (\Phi(A) - \Phi(C)) + (\Phi(C) - \Phi(B)) \quad (7.16)$$

for any triad of amplitudes A, B, C . As a result the relative unitary phases cannot be arbitrary but must form a self-consistent set satisfying (7.16). In addition, the relative phases must be in full accord with all measured interference terms. To build up such a self-consistent set we must start with the relative phases of S and P -wave amplitudes. For dipion masses $m \lesssim 980$ MeV the $S - P$ interference terms require

$$\Phi(U_{0\tau}^1) - \Phi(U_{0\tau}^0) = \Phi(L_\tau) - \Phi(S_\tau) = 0 \quad (7.17a)$$

$$\Phi(U_{0\tau}^1) - \Phi(U_{1\tau}^1) = \Phi(L_\tau) - \Phi(U_\tau) = +\pi \quad (7.17b)$$

$$\Phi(U_{1\tau}^1) - \Phi(U_{0\tau}^0) = \Phi(U_\tau) - \Phi(S_\tau) = -\pi \quad (7.17c)$$

where we have introduced an alternate notation for the S - and P -wave amplitudes that will be used in the following sections. These unitary phases define unitary phases in (7.14)

$$\Phi(U_{0\tau}^0) - \Phi(N_{1-\tau}^1) = \Phi(S_\tau) - \Phi(N_{-\tau}) = 0 \quad (7.18a)$$

$$\Phi(U_{0\tau}^1) - \Phi(N_{1-\tau}^1) = \Phi(L_\tau) - \Phi(N_{-\tau}) = 0 \quad (7.18b)$$

$$\Phi(U_{1\tau}^1) - \Phi(N_{1-\tau}^1) = \Phi(U_\tau) - \Phi(N_{-\tau}) = -\pi. \quad (7.18c)$$

In Table II we present an example of a complete set of self-consistent unitary phases arising from these initial unitary phases. The relative phases involving D -wave and higher spin waves are hypothetical since the corresponding interference terms have not yet been directly measured. In Table II we define the relative phase

$$\omega = \Phi(S_d) - \Phi(S_u) = -(\Phi(N_d) - \Phi(N_u)). \quad (7.19)$$

VIII. TEST OF THE UNITARY EVOLUTION LAW

A. Unitary amplitude analysis of the S - and P -wave subsystem at small t

For dipion masses $m \lesssim 1080$ MeV and momentum transfers $|t| \lesssim 0.20$ (GeV/c)² the S - and P -waves dominate the $\pi^- p \rightarrow \pi^- \pi^+ n$ process. Using Table I, the measured spin density matrix elements R_u^0 and R_y^0 organize into two groups of observables $a_{k,\tau}$, $k = 1, 6$ corresponding to target nucleon transversity $\tau = u$ and $\tau = d$. Their expressions in terms of transversity amplitudes in the notation introduced in the previous section are given in Table III together with the expressions for the measured elements R_x^0 . Omitting the subscript τ for the sake of brevity, we find from Table III

$$|S|^2 = a_1 + a_2 - 3|L|^2 \quad (8.1a)$$

$$|U|^2 = |L|^2 - \frac{1}{2}(a_2 + a_3) \quad (8.1b)$$

TABLE II. Self-consistent relative phases $\Phi(A) - \Phi(B)$ in bilinear products AB^* of unitary amplitudes $A = U_{0\tau}^J, U_{\lambda\tau}^J, N_{1\tau}^K, N_{\mu\tau}^K$ and $B = U_{0\tau}^{J'}, U_{\lambda'\tau}^{J'}, N_{1\tau}^{K'}, N_{\mu'\tau}^{K'}$ where $\lambda, \lambda' > 0$ and $\mu, \mu' > 1$. The superscripts J, J' and K, K' go with subscripts $0, \lambda, 0, \lambda'$ and $1, \mu, 1, \mu'$, respectively. The phase $\omega = \Phi(S_d) - \Phi(S_u)$.

AB^*	U_{0u}^*	$U_{\lambda'u}^*$	N_{1d}^*	$N_{\mu'd}^*$	U_{0d}^*	$U_{\lambda'd}^*$	N_{1u}^*	$N_{\mu'u}^*$
U_{0u}	0	π	0	π	$-\omega$	$-\omega + \pi$	$-\omega$	$-\omega + \pi$
$U_{\lambda u}$	$-\pi$	0	$-\pi$	0	$-\omega - \pi$	$-\omega$	$-\omega - \pi$	$-\omega$
N_{1d}	0	π	0	π	$-\omega$	$-\omega + \pi$	$-\omega$	$-\omega + \pi$
$N_{\mu d}$	$-\pi$	0	$-\pi$	0	$-\omega - \pi$	$-\omega$	$-\omega - \pi$	$-\omega$
U_{0d}	ω	$\omega + \pi$	ω	$\omega + \pi$	0	π	0	π
$U_{\lambda d}$	$\omega - \pi$	ω	$\omega - \pi$	ω	$-\pi$	0	$-\pi$	0
N_{1u}	ω	$\omega + \pi$	ω	$\omega + \pi$	0	π	0	π
$N_{\mu u}$	$\omega - \pi$	ω	$\omega - \pi$	ω	$-\pi$	0	$-\pi$	0

TABLE III. Measured spin observables for the S - and P -wave subsystem in terms of nucleon transversity amplitudes. The signs $+$ and $-$ correspond to $\tau = u$ and $\tau = d$, respectively. The superscripts $J = 0, 1$ are omitted. Real parts $\text{Re}R_k^0$, $k = u, y$ and imaginary parts $\text{Im}R_x^0$ are understood. The density matrix elements with subscripts SP and PP are defined by Eqs. (6.41).

$$\begin{aligned}
a_{1,\tau} &= \frac{1}{2}((R_u^0)_{SP} \pm (R_y^0)_{SP}) = |S_\tau|^2 + |L_\tau|^2 + |U_\tau|^2 + |N_\tau|^2 \\
a_{2,\tau} &= (R_u^0)_{PP} \pm (R_y^0)_{PP} = 2|L_\tau|^2 - |U_\tau|^2 - |N_\tau|^2 \\
a_{3,\tau} &= (R_u^0)_{1-1} \pm (R_y^0)_{1-1} = |N_\tau|^2 - |U_\tau|^2 \\
a_{4,\tau} &= \frac{1}{2}((R_u^0)_{0s} \pm (R_y^0)_{0s}) = |L_\tau||S_\tau| \cos(\Phi(L_\tau) - \Phi(S_\tau)) \\
a_{5,\tau} &= \frac{1}{\sqrt{2}}((R_u^0)_{01} \pm (R_y^0)_{01}) = |L_\tau||U_\tau| \cos(\Phi(L_\tau) - \Phi(U_\tau)) \\
a_{6,\tau} &= \frac{1}{\sqrt{2}}((R_u^0)_{1s} \pm (R_y^0)_{1s}) = |U_\tau||S_\tau| \cos(\Phi(U_\tau) - \Phi(S_\tau)) \\
r_1 &= \sqrt{2}(R_x^0)_{s1} = -\text{Re}(S_u N_d^*) + \text{Re}(N_u S_d^*) \\
r_2 &= \sqrt{2}(R_x^0)_{01} = -\text{Re}(L_u N_d^*) + \text{Re}(N_u L_d^*) \\
r_3 &= (R_x^0)_{-11} = +\text{Re}(U_u N_d^*) - \text{Re}(N_u U_d^*)
\end{aligned}$$

$$|N|^2 = |L|^2 - \frac{1}{2}(a_2 - a_3) \quad (8.1c)$$

$$|L|^2 = a_4 a_5 / (a_6 \Gamma) \quad (8.1d)$$

where

$$\Gamma = \frac{\cos(\Phi(L) - \Phi(S)) \cos(\Phi(L) - \Phi(U))}{\cos(\Phi(U) - \Phi(S))} = 1. \quad (8.2)$$

For all m below 1080 MeV $a_5 < 0$. For m below 980 MeV $a_4 > 0$ and $a_6 < 0$. These signs yield the phases (7.17) and (7.18). For m above 980 MeV $a_{4,d}$ and $a_{6,d}$ change signs prompting a change in relative phases

$$\Phi(L_d) - \Phi(S_d) = +\pi \quad (8.3a)$$

$$\Phi(L_d) - \Phi(U_d) = +\pi \quad (8.3b)$$

$$\Phi(U_d) - \Phi(S_d) = 0 \quad (8.3c)$$

and

$$\Phi(S_d) - \Phi(N_u) = -\pi \quad (8.4a)$$

$$\Phi(L_d) - \Phi(N_u) = 0 \quad (8.4b)$$

$$\Phi(U_d) - \Phi(N_u) = -\pi. \quad (8.4c)$$

The mixed sets of phases (7.17), (7.18) and (8.3), (8.4) for $\tau = u$ and $\tau = d$, respectively, still define a self-consistent set of relative phases. In all cases $\Gamma = 1$ so that the amplitudes $|L|^2$, and consequently all amplitudes in (8.1) as well, have a unique solution for both transversities. With $a_4 = |L||S|$ and $a_5 = \pm|L||U|$ we find from (8.1)

$$\begin{aligned}
a_2 &= -a_1 + 3|L|^2 + \frac{a_4^2}{|L|^2} \\
a_3 &= +a_1 - |L|^2 - \frac{a_4^2 + 2a_5^2}{|L|^2}. \quad (8.5)
\end{aligned}$$

These variables thus are not independent and must be calculated during the analysis and tested for their being within the error volume of the data.

B. Unique solution for unitary amplitudes

The amplitude analysis was carried out using a Monte Carlo method to search for physical solutions of amplitudes within the error volume of the data. The data were sampled using 10 million sampling data points. Initial analysis was unconstrained by fits to R_x^0 data and was followed by constrained analyses with fits to R_x^0 data constrained by 1, 3 and 5 standard deviations.

The unique solution for the moduli from the unconstrained analysis is shown in Figs. 1 and 2. The transversity “up” amplitudes are suppressed while the transversity “down” amplitudes dominate with a pronounced $\rho^0(770)$ peak. The data clearly require $\rho^0(770)$ in both S -wave amplitudes. There is a gap of no solution for masses 920–980 MeV in the $f_0(980)$ mass region suggesting the unitary phases are not compatible with $\rho^0(770) - f_0(980)$ mixing in the P -wave amplitude $|L_d|^2$ seen in the data in the previous analysis with nonunitary phases [13].

To test the rotational symmetry, and thus Lorentz symmetry, of the resonance production dynamics we need information on transversity amplitudes H_τ^λ with definite dipion helicity $\lambda = 0, \pm 1$. The transverse amplitudes U_τ and N_τ are a mix of transverse amplitudes with helicities

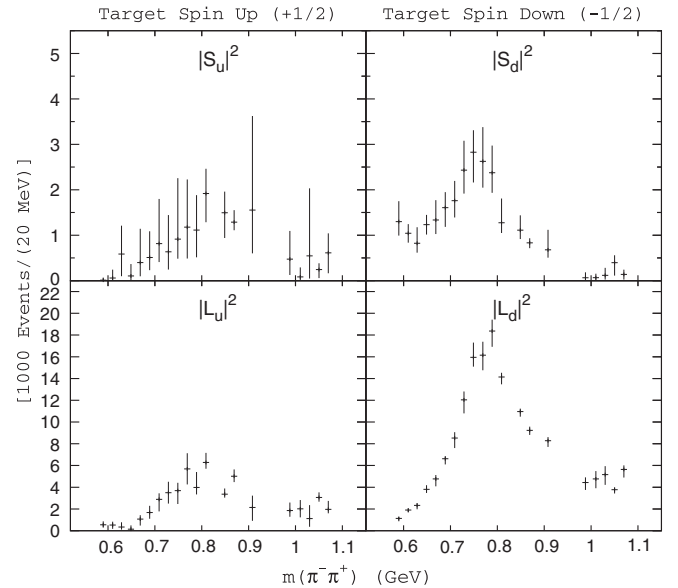


FIG. 1. S -wave and P -wave transversity amplitudes $|S_\tau|^2$ and $|L_\tau|^2$ from unitary amplitude analysis.

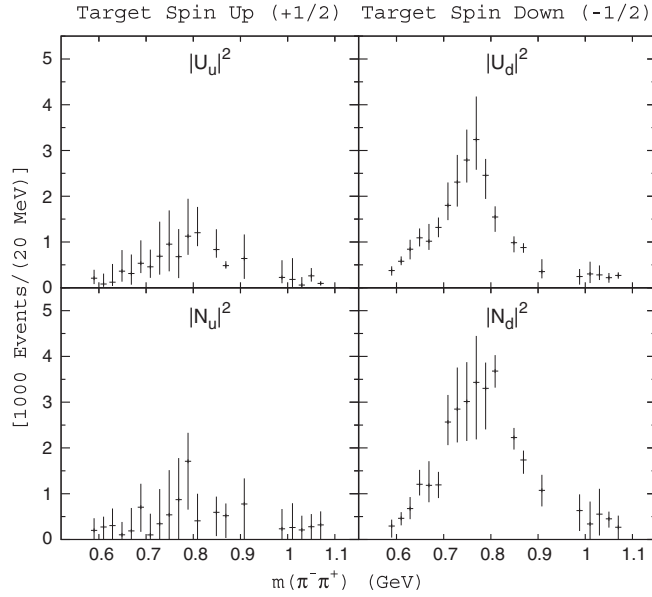


FIG. 2. P -wave transversity amplitudes $|U_\tau|^2$ and $|N_\tau|^2$ from unitary amplitude analysis.

$\lambda = \pm 1$ and are thus not suitable to test the symmetry. From (5.9) we find

$$H_\tau^{\pm 1} = \frac{1}{\sqrt{2}}(U_\tau \pm N_\tau). \quad (8.6)$$

Their partial wave intensities can be calculated from the data on polarized target

$$I(H_\tau) = |H_\tau^{+1}|^2 + |H_\tau^{-1}|^2 = |U_\tau|^2 + |N_\tau|^2. \quad (8.7)$$

In Fig. 3 we show the shape of the resonant peaks of $|U_\tau|^2$ and $|N_\tau|^2$. At half height the width of the $|U_d|^2$ peak is ~ 100 MeV while that of $|N_d|^2$ is ~ 180 MeV. This difference arises from the interference terms of amplitudes $H_d^{\pm 1}$

$$\begin{aligned} |U_d|^2 &= \frac{1}{2}(I(H_d) + P(H_d)) \\ |N_d|^2 &= \frac{1}{2}(I(H_d) - P(H_d)) \end{aligned} \quad (8.8)$$

where $P(H_d) = 2\text{Re}(H_d^{+1}H_d^{-1*}) = |U_d|^2 - |N_d|^2$. The figure shows the resonant shape of intensities $I(H_\tau)$. At half height the width of $I(H_d)$ is ~ 150 MeV—the proper width of $\rho^0(770)$ found also in the $\lambda = 0$ amplitude $|L_d|^2$. These results support the rotational/Lorentz symmetry of the resonance production dynamics.

C. Test of the unitary solution: Predictions for R_x^0

With unique moduli and unique phases (7.18) and (8.4), the unitary solution makes unique predictions for the measured elements R_x^0 given in Table III. For each sampling

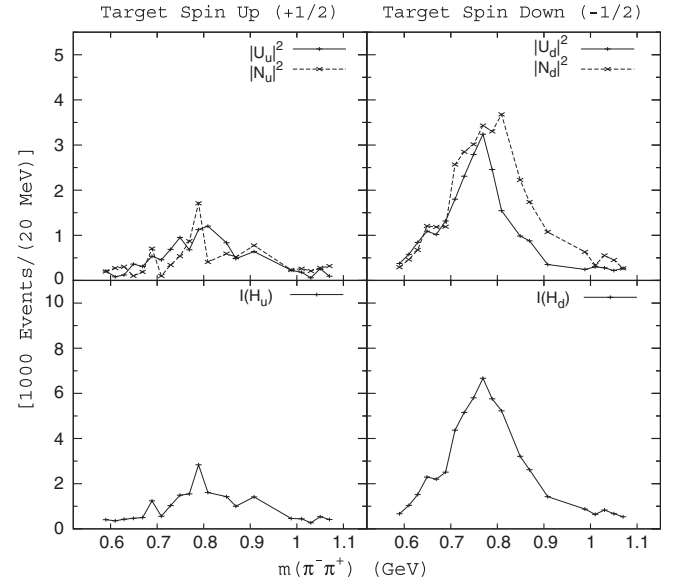


FIG. 3. The test of rotational/Lorentz symmetry of resonance production dynamics in $\pi^- p \rightarrow \pi^- \pi^+ n$ in amplitude analysis with unitary phases.

with a physical solution we calculated the elements R_u^0 , R_y^0 and R_x^0 . For these predicted values we calculated the corresponding value of χ^2 . From the distribution of the χ^2 values we calculated their range of values and the average in each mass bin. From these average values of χ^2 we calculated its bin-averaged χ^2 for each observable. In the case of R_u^0 and R_y^0 we further reduced the result to a more manageable average over the corresponding elements labeled $\chi^2(\langle R_u^0 \rangle)$ and $\chi^2(\langle R_y^0 \rangle)$, respectively. The goodness of the predictions is evaluated by (1) the number of empty mass bins with no physical solutions out of the total of 25 bins, (2) the average number of “pass” events (i.e. physical solutions) per bin, (3) the values of $\chi^2(\langle R_u^0 \rangle)$ and $\chi^2(\langle R_y^0 \rangle)$, and (4) the bin average values of χ^2 of the observables R_x^0 labeled $\chi^2((R_x^0)_{s1})$, $\chi^2((R_x^0)_{01})$ and $\chi^2((R_x^0)_{-11})$.

Table IV presents the results for 3 predictions. The first two predictions correspond to χ^2 of R_x^0 data constrained in each mass bin to within 3 and 5 standard deviations for each sampling with a physical solution for the moduli. The third prediction is the result of unconstrained analysis with no such constraints on χ^2 to R_x^0 data. All predictions for R_u^0 and R_y^0 have a good χ^2 . However, the first two predictions suffer from the large number of empty bins with no solution and a negligible number of constrained physical solutions in the remaining bins. The third prediction suffers from a very broad range of χ^2 values for R_x^0 data in each bin and from very large bin-averaged values. This χ^2 value is particularly large for the S -wave observable $(R_x^0)_{s1}$. We must conclude that the unitary solution is excluded by the R_x^0 data by at least 5 standard deviations.

TABLE IV. Three sets of predictions of unitary amplitude analysis with χ^2 for R_x^0 data constrained to within 3σ , 5σ and unconstrained. The notation is as defined in the text. The sampling size is 10 million data points.

Prediction	3σ	5σ	No constraint
Empty bins	11 of 25	9 of 25	5 of 25
Pass/bin	1	1	144, 227
$\chi^2(\langle R_u^0 \rangle)$	0.329	0.349	0.352
$\chi^2(\langle R_y^0 \rangle)$	0.316	0.329	0.383
$\chi^2(\langle R_x^0 \rangle_{s1})$	0.891	1.278	6.494
$\chi^2(\langle R_x^0 \rangle_{01})$	0.718	0.737	3.762
$\chi^2(\langle R_x^0 \rangle_{-11})$	0.689	0.681	2.156

D. The effect of dipion D -waves on a unique unitary solution

Measurements of $\pi N \rightarrow \pi\pi N$ do not measure the spin density matrix (SDM) elements $(R_k^0)_{\lambda\lambda'}^{JJ'}$ directly. Measurements on unpolarized targets measure moments t_M^L and measurements on polarized targets add moments p_M^L and r_M^L [24,51,53]. The moments t_M^L, p_M^L, r_M^L are expressed in terms of $(R_u^0)_{\lambda\lambda'}^{JJ'}, (R_y^0)_{\lambda\lambda'}^{JJ'}, (R_x^0)_{\lambda\lambda'}^{JJ'}$, respectively. Only the moments t_M^L and p_M^L with $L \leq 2$ involve S - and P -wave SDM elements but they also include $S-D$ - and $P-D$ -wave interference SDM elements. D -wave SDM elements contribute only to moments t_M^L and p_M^L with $L = 0, 3, 4$. There are $D-F$ interference terms in moments with $L = 3, 4$. Explicit formulas for t_M^L in terms of SDM elements are given in Ref. [54]. The observables $a_{k,\tau}, k = 1, 6$ and $r_\ell, \ell = 1, 3$ in Table III thus include, in general, also D -wave contributions.

Below the $K\bar{K}$ threshold for $m < 980$ MeV the D -wave moments with $L = 3, 4$ are very small compared to the S - and P -wave moments with $L = 1, 2$ with an exception of t_1^3 near 600–800 MeV (Fig. 14 of Ref. [54]). Since this observation holds true in all other measurements of $\pi^-\pi^+$ and $\pi^+\pi^-$ production, it is a common conclusion that for dipion masses $m < 980$ MeV at low t S - and P -wave amplitudes dominate and D -wave amplitudes can be neglected [6–16].

For $m > 980$ MeV at low t [from the $f_0(980)$ resonance] there is a sudden increase in the moments with $L = 3, 4$ and the D -waves can no longer be neglected. Measurements on polarized targets in fact enable us to determine the D -wave amplitudes (intensities) from 980–1600 MeV in 20 MeV bins. In the mass range $980 < m < 1080$ MeV the D -wave amplitudes are still relatively small compared to the P -wave which enables us to make a crude approximation of the S - and P -wave dominance even in this mass range. Figure 1 in Ref. [8] shows that the ratio of the D -wave intensities to the sum of the S - and P -wave intensities is 0.37 at 990 MeV and 0.47 at 1070 MeV. Since it is not possible to determine an exact analytical solution for the D -wave amplitudes

in terms of the measured polarization data certain approximations must be made in these analyses.

There are five D -wave transversity amplitudes: three unnatural exchange amplitudes $D_\tau^0, D_\tau^U, D_\tau^{2U}$ with helicities $\lambda = 0, 1, 2$ and two natural exchange amplitudes D_τ^N, D_τ^{2N} with helicities $\lambda = 1, 2$. The observables $a_{k,\tau}, k = 1, 6$ and $r_\ell, \ell = 1, 3$ can be written in the form

$$a_{k,\tau} = c_{k,\tau} + d_{k,\tau} + e_{k,\tau}$$

$$r_\ell = r_\ell(SP) + r_\ell(D) \quad (8.9)$$

where the $c_{k,\tau}$ are the S - and P -wave terms given in Table III, $d_{k,\tau}$ are D -wave terms involving D -wave amplitudes with $\lambda \leq 1$ and $e_{k,\tau}$ are terms involving $\lambda = 2$ amplitudes. Similarly, $r_\ell(SP)$ involve only the S - and P -wave terms given in Table III and $r_\ell(D)$ include D -waves. The expressions for $d_{k,\tau}, e_{k,\tau}, r_\ell(D)$ in terms of the transversity amplitudes are given in Refs. [24,53].

We wish to quantify the effect of the D -waves on the unitary amplitude analysis, both constrained and unconstrained. In our new analysis we shall neglect the smallest D -wave amplitudes D^{2U} and D^{2N} and set $e_{k,\tau} = 0$. For all relative phases we assume the consistent unitary phases given in Table II with the modifications (8.3) and (8.4). For the moduli $|D_\tau^0|, |D_\tau^U|, |D_\tau^N|$ we shall use a series of estimates obtained as follows to study the response of the unitary amplitudes.

For dipion masses $m > 980$ MeV we know the D -wave intensities $I(A) = |A_u|^2 + |A_d|^2, A = D^0, D^U, D^N$ from the amplitude analysis of the CERN measurement [8]. We have linearly extrapolated these intensities from their values $I_2(A)$ at $m_2 = 990$ MeV to value $I_1(A) = TI_2(A)$ at $m_1 = 590$ MeV where the fraction T defines the slope parameter. The extrapolated intensities at mass m are

$$I(A, m) = TI_2(A) + \frac{(1-T)I_2(A)}{m_2 - m_1}(m - m_1). \quad (8.10)$$

Below 980 MeV there is a fairly constant ratio of the moduli $|A_u|^2 : |A_d|^2 \approx 1:3$ for all S - and P -wave amplitudes. Using this ratio we have reconstructed the moduli of the D -wave amplitudes from the intensities

$$|A_u(m)|^2 = 0.25I(A, m)F$$

$$|A_d(m)|^2 = 0.75I(A, m)F \quad (8.11)$$

where the factor F accounts for the sudden decrease of D -wave moments below 980 MeV. We varied the slope parameter T in the range from 0.05 to 0.75 to estimate the D -wave amplitudes below 980 MeV. Above 980 MeV we have used the amplitudes (8.11) calculated from the measured intensities of the analysis [8]. The analysis was performed for $F = 1.00$ and for $F = 0.50$. We have used the conversion factor $0.109 \mu b/20$ MeV = 1000 Events/20 MeV to convert the units of Ref. [8] to units of Ref. [54] used in our analysis.

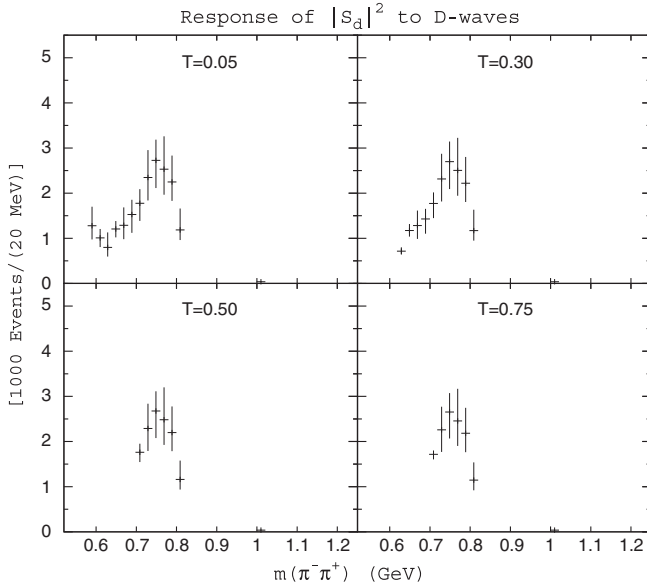


FIG. 4. Response of the amplitude $|S_d|^2$ to D -wave amplitudes in unitary analysis assuming $F = 1.00$.

To accommodate the interference terms between the D -wave amplitudes and S - or P -wave amplitudes we used a form of a perturbation theory. Our code first calculated the unitary analysis assuming $c_{k,\tau} = a_{k,\tau}$ and, independently, the extrapolation of the D -wave amplitudes. The resulting S - and P -wave amplitudes were used to calculate the terms $d_{k,\tau}$. Then new “perturbed” $c_{k,\tau} = a_{k,\tau} - d_{k,\tau}$ were used to calculate new unitary S - and P -wave amplitudes to see their response to the presumed absence of the D -waves in the new parameters $c_{k,\tau}$.

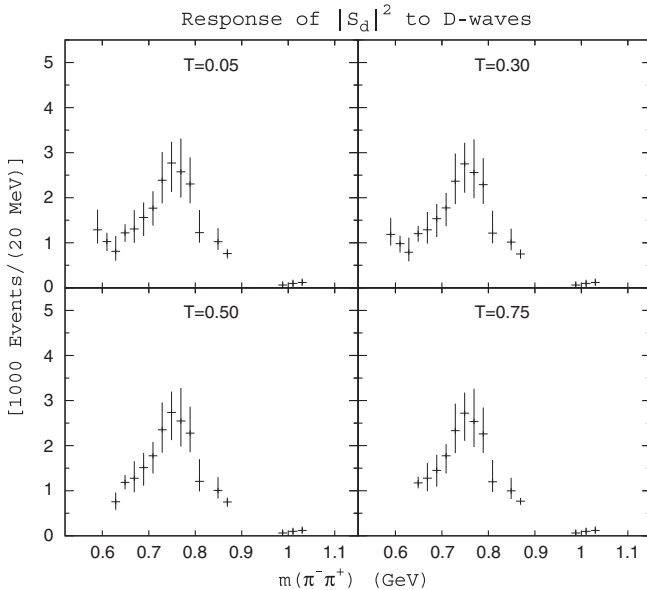


FIG. 5. Response of the amplitude $|S_d|^2$ to D -wave amplitudes in unitary analysis assuming $F = 0.50$.

TABLE V. Four sets of predictions of unitary amplitude analysis including dipion D -waves D^0, D^U, D^N assuming $F = 0.50$ with χ^2 for R_x^0 data constrained to within 5σ and unconstrained for parameters $T = 0.05$ and $T = 0.75$. The notation is as defined in the text. The sampling size is 10 million data points.

Prediction	5σ	5σ	No constraint	No constraint
T	0.05	0.75	0.05	0.75
Empty bins	12 of 25	14 of 25	8 of 25	11 of 25
Pass/bin	1	106	121 190	80 498
$\chi^2((R_u^0))$	0.379	0.380	0.351	0.370
$\chi^2((R_y^0))$	0.360	0.365	0.383	0.394
$\chi^2((R_x^0)_{s1})$	1.776	1.379	5.112	4.501
$\chi^2((R_x^0)_{01})$	0.966	1.024	3.948	3.643
$\chi^2((R_x^0)_{-11})$	0.830	0.641	2.452	2.601

The results for the critical amplitude $|S_d|^2$ from the unconstrained analysis with $F = 1.00$ at $T = 0.05, 0.30, 0.50, 0.75$ are shown in Fig. 4. There are no physical solutions for $m > 800$ MeV and for $m < 700$ MeV for $T = 0.50$ and $T = 0.75$ while there is only a little change in the $\rho^0(770)$ mass region at all T . These results suggest that the D -wave contribution is overestimated in this unitary amplitude analysis which motivates us to consider the case $F = 0.50$.

The results for the critical amplitude $|S_d|^2$ from the unconstrained analysis with $F = 0.50$ at $T = 0.05, 0.30, 0.50, 0.75$ are shown in Fig. 5. Apart from an increase of empty bins from 5 to 8–11 at masses away from the $\rho^0(770)$ mass, this amplitude shows only a very weak response to D -waves at all T . In particular, there is no change in the presence of the $\rho^0(770)$ resonance in the S -wave.

Table V quantifies the responses of the unitary analysis with $F = 0.50$ constrained by 5σ fits to the data on SDM elements R_x^0 and of the analysis unconstrained by such fits. In the unconstrained analysis there is a modest improvement in χ^2 for $(R_x^0)_{s1}$ but which remains still too high. The constrained analysis has a higher number of empty bins at all T than the constrained analysis without D -waves and a similarly negligible number of physical solutions per bin. On this basis we conclude that the unitary solution is excluded at the 5σ level with or without the D -wave contributions in the input data.

IX. EVIDENCE FOR THE QUANTUM ENVIRONMENT AND ITS PURE DEPHASING INTERACTION WITH PARTICLE SCATTERING PROCESSES

A. The hypothesis of the quantum environment

In the Introduction we have put forward a hypothesis that the physical Universe includes a quantum environment which interacts with some particle scattering and decay processes. To be consistent with the conservation laws of the Standard Model this new interaction must be a pure

dephasing interaction of the produced S -matrix final state $\rho_f(S)$ with quantum states $\rho(E)$ of the environment. It manifests itself by modifying (dephasing) the phases of the S -matrix amplitudes in a nonunitary evolution of the produced final state $\rho_f(S)$ to the observed final state $\rho_f(O)$ given by the Kraus representation.

The most general form of Kraus representation reads

$$\rho_f(O) = \sum_{k=1}^M A_k \rho_f(S) A_k^\dagger. \quad (9.1)$$

In quantum theory the nonunitary evolution law (9.1) can be always derived from a unitary coevolution of the initial quantum system S_i with a quantum environment E by tracing out the environment in the joint final state $\rho_f(S_f, E)$. The unitary evolution is given by

$$\rho_f(S_f, E) = U \rho(E) \otimes \rho(S_i) U^\dagger \quad (9.2)$$

where the quantum state(s) of the environment are described by the density matrix [17,53]

$$\rho(E) = \sum_{m,n} p_{mn}(E) |e_m\rangle \langle e_n|. \quad (9.3)$$

Here $|e_m\rangle, m = 1, M$ are M orthonormal eigenstates describing the interacting degrees of freedom of the environment. Their number is limited by the dimensions of the Hilbert spaces [3]

$$M = \dim H(E) \leq \dim H(S_i) \dim H(S_f). \quad (9.4)$$

Assuming the conservation of the quantum numbers of the states $|e_m\rangle$ by the evolution operator

$$\langle e_k | U | e_m \rangle = \delta_{km} \langle e_k | U | e_k \rangle = \delta_{km} V_k \quad (9.5)$$

the trace $\rho(S_f) = \text{Tr}_E \rho_f(S_f, E)$ reads

$$\rho(S_f) = \sum_{k=1}^M p_{kk} V_k \rho(S_i) V_k^\dagger. \quad (9.6)$$

In particle scattering processes we use the notation $\rho(S_i) = \rho_i(S)$ and $\rho(S_f) = \rho_f(O)$.

Given (9.1) we can always enlarge the Hilbert space $H(S_i)$ to $H(E) \otimes H(S_i)$ with $\dim H(E) = M$, define a unitary evolution of this system and recover (9.6) as a trace over the ‘‘quantum environment’’ $H(E)$. Given (9.6) we always recover (9.1) with the replacement

$$\sqrt{p_{kk}} V_k \equiv A_k. \quad (9.7)$$

The two forms of the nonunitary evolution are equivalent provided M satisfies (9.4). The quantum environment can be either an ancillary nonphysical (mathematical) quantum

environment, or it can be a real physical quantum environment [3]. Any interaction of a physical environment with a quantum system is described by (9.6).

B. The evidence for a pure dephasing nonunitary evolution in $\pi N \rightarrow \pi\pi N$

The existence of a physical quantum environment and its pure dephasing interaction with particle scattering is supported by the following chain of evidence for the nonunitary evolution in $\pi N \rightarrow \pi\pi N$ processes and its dephasing character. We assume the nonunitary evolution law (9.1) without a reference to quantum environment but the evidence applies equally well for the nonunitary evolution law (9.6) assuming interaction with the quantum environment.

1. The observed amplitudes are not S -matrix amplitudes

Amplitude analysis of the S - and P -wave subsystem with unitary relative phases yields a unique solution from the data on the observables R_u^0 and R_y^0 which fails to fit the experimental data on the observables R_x^0 at the 5σ level. The moduli of the transversity amplitudes in this analysis are nearly identical to the moduli found in amplitude analyses without unitary phases. There is therefore only one reason for this failure: the unitary relative phases. This means that the partial wave amplitudes describing the CERN data cannot be the S -matrix amplitudes and must have nonunitary phases.

2. Nonunitary evolution is involved in the $\pi N \rightarrow \pi\pi N$ processes

All previous amplitude analyses of the S - and P -wave subsystem in $\pi^- p \rightarrow \pi^- \pi^+ n$ at 17.2 GeV/c [6–15] and at 1.78 GeV/c [16] as well as in $\pi^+ n \rightarrow \pi^+ \pi^- p$ at 5.98 and 11.85 GeV/c [10–12] found nonunitary relative phases Φ_{LS}, Φ_{LU} and Φ_{US} . The analyses [6–9] and the extension [55] of recent analyses Refs. [13,15] included the data on R_x^0 in their fits. The analyses of the S, P, D and S, P, D, F subsystems yield nonunitary relative phases at higher dipion masses and momentum transfers [7–9]. Recent amplitude analysis of $\pi^- p \rightarrow \pi^0 \pi^0 n$ at 18.3 GeV/c also found nonunitary phases [56]. The contrast between the predicted unitary relative phases and the observed nonunitary phases presents unambiguous evidence for a dephasing nonunitary evolution involved in the $\pi N \rightarrow \pi\pi N$.

3. The nonunitary evolution evolves the produced final state $\rho_f(S)$ into the observed state $\rho_f(O)$

The evidence for this claim comes from two independent features of the observed amplitudes.

- (i) In Ref. [24] we present a survey of S -wave moduli and intensities from all amplitude analyses of the five measurements of $\pi^- p \rightarrow \pi^- \pi^+ n$ and $\pi^+ n \rightarrow \pi^+ \pi^- p$ on polarized targets. All these analyses

provide remarkably consistent evidence for a rho-like state in the S -wave of these processes which is not seen in the $\pi^- p \rightarrow \pi^0 \pi^0 n$ amplitude analysis of the high statistics measurement at 18.3 GeV/c [56]. In Ref. [15] we identify this rho-like state with $\rho^0(770)$ resonance indicating a $\rho^0(770) - f_0(980)$ spin mixing in the S - and P -wave subsystem. As is the case with $\rho^0(770) - \omega(782)$ isospin mixing, the $\rho^0(770) - f_0(980)$ spin mixing requires a spin mixing interaction. Since there is no spin mixing interaction in the Standard Model, this nonstandard interaction must originate in the nonunitary evolution involved in the $\pi^- N \rightarrow \pi^- \pi^+ N$ processes.

- (ii) The analyses [13,15] established that the mass and the width of the $\rho^0(770)$ resonance Breit-Wigner peak observed in all P -wave amplitudes do not depend on its helicity λ as required by the rotational/Lorentz symmetry of the S -matrix. These results are similar to the results of the unitary analysis shown in Fig. 3.

These two findings imply that the resonance production and the spin mixing have separate dynamical origins. There is no reason to assume that the production process is described by anything other than the S -matrix dynamics. While the observed amplitudes reveal nonunitary spin mixing, they are also consistent with the Lorentz symmetric S -matrix dynamics and its unitary evolution law. This is possible if and only if the nonunitary evolution evolves the produced final state $\rho_f(S)$ into the observed final state $\rho_f(O)$ as described by the Kraus representation (9.1) or (9.6). The dephasing nonunitary evolution is then a final state evolution described by the amplitudes of the Kraus operators.

4. The nonunitary evolution is a pure dephasing evolution

We now show that the nonunitary evolution is a pure (nondissipative) dephasing evolution. Suppose such is not the case and the evolution is dissipative. As the result of the exchange of the four-momentum of the final state particles with the environment there is no conservation of the total four-momentum. As a result the measured four-momenta of the two produced pions will no longer be able to generate the Breit-Wigner shape of produced resonances in the observed amplitudes. There is also a breakdown of the conservation of the total angular momentum due to the exchange of angular momentum with the environment leading to the breaking of rotational and Lorentz symmetry by the produced resonances. The observed mass and the width of the distorted resonance like $\rho^0(770)$ will depend on its helicity, contrary to the observations. We must conclude that the nonunitary evolution (9.1) or (9.6) is a pure dephasing evolution that leaves all four-momenta of the final state particles intact.

C. Evidence for a physical quantum environment

The hypothesis of the existence of the quantum environment is validated (A) by the necessity to explain the physical origin of the nonunitary evolution as a physical process and (B) by identifying the quantum environment as a component of dark matter in a plausible model.

1. The nonunitary evolution as a physical process

A nonunitary evolution of a quantum system described by (9.1) by itself does not necessarily require an interaction of the system with a physical environment. The chief difference between the nonunitary evolution law (9.1) and (9.6) is that the Kraus operators A_k in (9.1) describe only the nonunitary evolution of the quantum system. In this form Kraus operators lack any other physical meaning and there is no physical limit on their number M . As well in this case the nonunitary evolution has no explicit physical origin. In contrast the Kraus operators V_k in (9.6) describe both the nonunitary evolution of the system and its interaction with the environment which gives them a clear physical meaning. In this case the nonunitary evolution is generated by the interaction of the quantum system with the quantum environment.

The observed non- S -matrix amplitudes are a result of the nonunitary evolution law given by (9.1) or (9.6) and carry information about a new physics beyond the Standard Model. The nonunitary phases and spin mixing are generated by the Kraus operators A_k or V_k and are specific signatures of this new physics. We expect that the new physics originates in a new physical process, not in abstract operators like A_k that lack a clear physical meaning and whose number M is not physically restricted. This is particularly desirable in the case of the $\rho^0(770) - f_0(980)$ spin mixing which implies spontaneous violation of rotational/Lorentz symmetry in the observed S - and P -wave amplitudes [17]. We expect such an important new physical effect to have a new physical origin.

The experimental evidence presented in the preceding section does not distinguish between the nonunitary evolution law (9.1) without a reference to quantum environment and the nonunitary evolution law (9.6) generated by the interaction of the final state $\rho_f(S)$ with the quantum environment. However, when we impose the condition (9.4) on the dimension M then the nonunitary evolution law (9.1) is entirely equivalent to the nonunitary law (9.6) and we are free to describe the nonunitary evolution as an interaction of the system with a quantum environment. This enables us to identify the new physical process and its new physics with the new pure dephasing interaction with the environment.

In the sequel paper [17] we show that the consistency of the pure dephasing interaction with the symmetries and conservation laws of the Standard Model in $\pi N \rightarrow \pi\pi N$ processes requires that it be a dipion spin mixing interaction. Its effect is the mixing of S -matrix partial wave

amplitudes with different spins to form new observable partial wave amplitudes. The theory predicts $\rho^0(770) - f_0(980)$ spin mixing in the S - and P -wave amplitudes in $\pi^- p \rightarrow \pi^- \pi^+ n$ in excellent qualitative agreement with the experimental results [13,15]. Quantitative agreement with the CERN data is presented in the new analysis using a spin mixing mechanism [53]. The consistency of this new interaction with the Standard Model also supports the necessity for a physical process behind the nonunitary evolution and thus for a physical quantum environment.

Kraus operators must inform us about such a new process. They can only do so if they are interpreted as matrix elements $V_k = \langle e_k | U | e_k \rangle$ describing a coevolution of the state $\rho_f(S)$ with the physical quantum environment in terms of its interacting degrees of freedom. What also distinguishes (9.6) from (9.1) is the explicit presence of the information about the quantum environment in (9.6) in terms of the probabilities $p_{kk}, k = 1, M$. As a result the nonunitary evolution law must take the form (9.6) generated by a physical pure dephasing interaction of the produced state $\rho_f(S)$ with the quantum state $\rho(E)$ of the environment.

2. Physical nature of the quantum environment: Dark matter

The necessary and sufficient condition for the quantum environment to be a real physical environment is that its interacting degrees with the quantum system be physical interacting degrees of freedom, not ancillary ones. Then the pure dephasing interaction of the quantum system with the quantum environment will be also a real physical interaction. To validate the hypothesis of the existence of the quantum environment we need to identify the physical degrees of freedom of the environment which will also identify the process that generates the nonunitary evolution.

The consistency of the pure dephasing interaction with the particle Standard Model suggests that the quantum environment has a universal presence in the Universe which manifests itself in astrophysical observations. Astrophysical observations provide convincing evidence for the existence of dark matter and dark energy which are omnipresent environments in the Universe. Dark matter is characterized by nonstandard interactions with baryonic matter. The quantum environment is characterized by mixed quantum states $\rho(E)$ given by (9.3) where the eigenstates $|e_m\rangle$ describe its interacting degrees of freedom. The pure dephasing interaction is also a nonstandard interaction between the produced states $\rho_f(S)$ and the quantum states $\rho(E)$. In this aspect there is an obvious similarity between the dark matter and the quantum environment.

It is our conjecture that the quantum states $\rho(E)$ are particles of a distinct component of cold dark matter and that the pure dephasing interactions are its interactions with baryonic matter. The eigenstates $|e_k\rangle$ could represent some

new physical interacting degrees characterizing this component of dark matter and its nonstandard interactions with baryonic matter. But particle physics already knows of physical eigenstates with nonstandard interactions: neutrino mass eigenstates. In Ref. [53] we find that the dimension $M = 4$. This provides a specific physical motivation to identify the four eigenstates $|e_m\rangle$ with the four neutrino mass eigenstates $|m_k\rangle$ including the new presumed light mass eigenstate $|m_4\rangle$. We refer to the mixed states $\rho(E)$ as dark neutrinos. In contrast the three active neutrinos ν_e, ν_μ, ν_τ of the Standard Model and the new light sterile neutrino ν_s are pure states. All neutrinos engage in dephasing interactions and form the quantum environment. The light sterile neutrino background can be interpreted as hot dark matter.

Hot dark neutrinos were created in dephasing interactions of all flavor neutrinos with a variety of scattering processes in the early Universe and then redshifted to form warm and then a late cold component of cold dark matter. A careful analysis of the formation of galactic and large scale structures in the Universe indicates that most dark matter should be cold or warm at the onset of the galaxy formation when the temperature of the Universe was about 1 keV. At these temperatures dark neutrinos still formed a hot dark matter and thus can account for only a part of the dark matter. A possible candidate for warm dark matter is a sterile neutrino with mass 7.1 keV produced via lepton-number driven Mikheev-Smirnov-Wolfenstein resonant conversion of active neutrinos near or at the big bang nucleosynthesis epoch [57,58]. These sterile neutrinos are predicted to have a two-photon x-ray radiative decay at 3.55 keV [59,60]. An emission line at 3.55–3.57 keV was recently detected in the x-ray spectrum of galaxy clusters in two independent observations [61,62]. These results suggest a multicomponent neutrino structure of dark matter with dark neutrinos being one such component.

Interpreting the quantum environment as a component of dark matter endows it with a physical and material identity. The nonunitary evolution is generated by the interaction of the produced final states $\rho_f(S)$ with the cold dark neutrino component of dark matter and the light sterile and active neutrino backgrounds. We elaborate on this model of the quantum environment in Ref. [53].

X. A PHYSICAL INTERPRETATION OF THE UNITARY AND NONUNITARY RELATIVE PHASES

It follows from the unitary conditions (7.14) and (7.15) that all unnatural exchange amplitudes $U_{\lambda\tau}^J$ as well as all natural exchange amplitudes $N_{\lambda\tau}^J$ share the same absolute phase up to an integer multiple of π

$$\begin{aligned}\Phi(U_{\lambda\tau}^J) &= \Phi(S_\tau) + \pi n(U_{\lambda\tau}^J) \\ \Phi(N_{\lambda\tau}^J) &= \Phi(N_\tau) + \pi n(N_{\lambda\tau}^J).\end{aligned}\quad (10.1)$$

The unitary relative phases thus imply that if there is a resonance at mass m_R in a partial wave with $J = J_R$, then all contributing partial waves will have the same resonant phase near m_R . Mathematically, this does not necessarily imply that any of the partial waves with $J \neq J_R$ must resonate and show a resonant peak or a dip since the nonresonant moduli can still have resonant phases. Although the conditions (7.13) appear to allow such resonance mixing, it is excluded by the symmetries of the S -matrix.

The S -matrix amplitudes have a general form

$$\begin{aligned} U_{\lambda\tau}^J &= \exp \Phi(S_\tau) [(-1)^{n(U_{\lambda\tau}^J)} |U_{\lambda\tau}^J| + i0] \\ N_{\lambda\tau}^J &= \exp \Phi(N_\tau) [(-1)^{n(N_{\lambda\tau}^J)} |N_{\lambda\tau}^J| + i0]. \end{aligned} \quad (10.2)$$

The phases $\Phi(S_\tau)$ and $\Phi(N_\tau)$ are functions of energy s , momentum transfer t and dipion mass m . Near the resonant mass m_R the phases give rise to the usual form of the partial wave amplitudes $A_{\lambda\tau}^J$ with $J = J_R$ in terms of Breit-Wigner amplitudes $a_{\text{BW}}^{J_R}(m)$ and a complex background $B_{\lambda\tau}^{J_R}$

$$A_{\lambda\tau}^{J_R} = \langle \pi^- \pi^+, J_R \lambda | T | R, \lambda \rangle a_{\text{BW}}^{J_R}(m) \langle R, \lambda \tau_n | T | 0 \tau \rangle + B_{\lambda\tau}^{J_R} \quad (10.3)$$

where R is the resonance and T is the transition matrix which describes the production and subsequent decay of the resonance R in the partial wave amplitude $A_{\lambda\tau}^{J_R}$. The production and decay processes respect the conservation laws of the Standard Model within the amplitude $A_{\lambda\tau}^{J_R}$.

The unitary relative phases of the S -matrix amplitudes and the nonunitary relative phases of the observed amplitudes may have a simple and interesting physical interpretation. Consider complex standing waves on a string of the length L

$$y_n(x, t) = A_n(x) \cos(\omega_n t) = a_n \exp(ik_n x) \cos(\omega_n t) \quad (10.4)$$

arising from the superposition of two complex waves

$$y_n(x, t) = a_n \exp i(k_n x - \omega_n t) + a_n \exp i(k_n x + \omega_n t) \quad (10.5)$$

where the integer $n \geq 1$. With the wavelength $\lambda_n = n/2L$ the wave number $k_n = 2\pi/\lambda_n = \pi n/L$. With tension F and linear mass density of the string μ the angular frequency $\omega_n = (n/2L)\sqrt{F/\mu}$. The amplitude a_n may depend on ω_n . The real part $\text{Re}y_n(x, t)$ and the imaginary part $\text{Im}y_n(x, t)$ correspond to standing waves on the string open and closed at both ends, respectively,

$$\begin{aligned} \text{Re}y_n(x, t) &= a_n \cos(k_n x) \cos(\omega_n t) \\ \text{Im}y_n(x, t) &= a_n \sin(k_n x) \cos(\omega_n t). \end{aligned} \quad (10.6)$$

At the far end $x = L$ the phase of the standing wave is given by $\Phi_n = k_n L = n\pi$. At $x = L$ the relative phases of the standing waves are

$$\Phi_n - \Phi_m = (n - m)\pi = 0, \pm\pi, \pm 2\pi, \dots \quad (10.7)$$

and their wave functions $y_n(L, t)$ are

$$y_n(L, t) = \cos(\omega_n t) [(-1)^n |A_n(L)| + i0]. \quad (10.8)$$

A vibrating string in a vacuum (an empty space) does not generate sound waves. In a medium the vibrating string generates sound waves of the frequency ω_n but the sound waves are no longer standing waves. As a result two sound waves with frequencies ω_n and ω_m will no longer have a relative phase $(n - m)\pi$ as the wavelength changes in the medium. The relative phases will change for the sound waves in the medium.

The unitary relative phases of the S -matrix partial wave amplitudes $U_{\lambda\tau}^J$ and $N_{\lambda\tau}^J$ have the same relative phases as the vibrating string at $x = L$. We can write (10.2) for $U_{\lambda\tau}^J$ in the form

$$\begin{aligned} \text{Re}U_{\lambda\tau}^J &= \cos \Phi(S_\tau) [(-1)^{n(U_{\lambda\tau}^J)} |U_{\lambda\tau}^J| + i0] \\ \text{Im}U_{\lambda\tau}^J &= \sin \Phi(S_\tau) [(-1)^{n(U_{\lambda\tau}^J)} |U_{\lambda\tau}^J| + i0] \end{aligned} \quad (10.9)$$

and similarly for $N_{\lambda\tau}^J$. The comparison of (10.9) and (10.8) suggests the real and imaginary parts of these partial wave amplitudes are both akin to complex standing waves on strings open and closed at both ends. This similarity suggests to consider the S -matrix partial wave amplitudes as representations of some kind of complex dynamical (vibrational) modes confined to a finite dynamical region of a transient compound state. The modes are associated with the produced partial waves $|p_c p_d, J\lambda, \tau\rangle$. In empty space these partial waves propagate without a change leaving the S -matrix amplitudes intact. In the presence of a quantum environment the propagating partial waves $|p_c p_d, J\lambda, \tau\rangle$ are modified by the environment. This results in the modification of the S -matrix partial wave amplitudes into the observed partial wave amplitudes with the ensuing non-unitary relative phases. The quantum environment is responsible not only for the generation of the nonunitary phases but also for the observed $\rho^0(770) - f_0(980)$ mixing [17,24,53].

XI. CONCLUSIONS AND OUTLOOK

We have presented a spin formalism that allowed us to construct the full final state density matrix $\rho_f(S)$ in $\pi N \rightarrow \pi\pi N$ processes in S -matrix theory. We have shown that the unitary evolution law imposes specific constraints on the

relative phases of the transversity amplitudes $U_{\lambda\tau}^J$ and $N_{\mu\tau}^J$. The contrast between these predicted phases and the observed phases in all amplitude analyses of the pion production process presents an apparent violation of the unitary evolution law. Previous attempts to test unitary evolution law were framed as the test of the quantum mechanics itself. The central idea of this work is that an apparent violation of the unitary evolution law does not signal the breakdown of quantum theory. Rather it is unambiguous evidence for a nonunitary evolution of the produced final state $\rho_f(S)$ to the observed final state $\rho_f(O)$ generated by a new interaction of the state $\rho_f(S)$ with a quantum environment. To render the production mechanism accessible to experimental observation and to be consistent with the Standard Model this new interaction must be a pure dephasing interaction. This new nonstandard dynamics represents a new physics beyond the Standard Model.

We identify the quantum environment with dark neutrinos which form a distinct component of dark matter. This interpretation endows the quantum environment with a physical and material identity which connects it to the physics of the dark sector of the Universe. Parts of the quantum environment are also the active and light sterile

neutrino backgrounds. We elaborate on this model of the quantum environment in Ref. [53].

The spin formalism developed in this work and its consequences for the unitary phases of partial wave amplitudes apply equally well to a number of other meson production processes such as $KN \rightarrow K\pi N$, $\pi N \rightarrow \pi K\Lambda$, $\bar{K}N \rightarrow \pi\pi\Lambda$ and others. These processes could be measured on polarized target and the measurements with Λ would also allow measurements of recoil Λ polarization by its weak decays. Modern polarized targets reach high values of polarization and enable us to select an arbitrary direction of the polarization vector [50]. Such experiments would provide new and independent tests of the unitary evolution law and advance our understanding of the quantum environment and its pure dephasing interactions with particle scattering processes.

APPENDIX: PROOF OF THE UNITARY EVOLUTION CONSTRAINTS ON PARITY CONSERVING TRANSVERSITY AMPLITUDES

The unitary evolution constraints (7.12) on parity conserving transversity amplitudes follow from the constraint $A_{xx} = -A_{uu}$ which we can write in the form

$$(I_x^1)^2 + (I_x^3)^2 + (I_u^2)^2 - (I_u^0)^2 = -(I_u^1)^2 - (I_u^3)^2 - (I_x^2)^2 + (I_x^0)^2. \quad (\text{A1})$$

Expansions of the intensities involve $\text{Re}(Y_\lambda^J Y_{\lambda'}^{J'*})$ and $\text{Im}(Y_\lambda^J Y_{\lambda'}^{J'*})$ on the lhs and rhs of (A1), respectively. Using the expressions for R_k^J in Table I in the intensities (6.32) and (6.33), relabeling of some terms, parity relations (5.16), and a relation for spherical harmonics $Y_{-M}^L(\theta, \phi) = (-1)^M (Y_M^L(\theta, \phi))^*$, the intensities on the lhs of (A1) read

$$\begin{aligned} I_x^1 &= -2 \sum_{J,\lambda \geq 0} \sum_{J',\lambda' \geq 0} \eta_\lambda \eta_{\lambda'} (\xi_\lambda \xi_{\lambda'} \text{Re}(U_{\lambda u}^J U_{\lambda' d}^{J'*}) \text{Re} Y_\lambda^J \text{Re} Y_{\lambda'}^{J'} - 4 \text{Re}(N_{\lambda u}^J N_{\lambda' d}^{J'*}) \text{Im} Y_\lambda^J \text{Im} Y_{\lambda'}^{J'}) \\ I_x^3 &= +2 \sum_{J,\lambda \geq 0} \sum_{J',\lambda' \geq 0} \eta_\lambda \eta_{\lambda'} (\xi_\lambda \xi_{\lambda'} \text{Im}(U_{\lambda u}^J U_{\lambda' d}^{J'*}) \text{Re} Y_\lambda^J \text{Re} Y_{\lambda'}^{J'} + 4 \text{Im}(N_{\lambda u}^J N_{\lambda' d}^{J'*}) \text{Im} Y_\lambda^J \text{Im} Y_{\lambda'}^{J'}) \\ I_u^2 &= \sum_{J,\lambda \geq 0} \sum_{J',\lambda' \geq 0} \eta_\lambda \eta_{\lambda'} (\xi_\lambda \xi_{\lambda'} (\text{Re}(U_{\lambda u}^J U_{\lambda' u}^{J'*}) - \text{Re}(U_{\lambda d}^J U_{\lambda' d}^{J'*})) \text{Re} Y_\lambda^J \text{Re} Y_{\lambda'}^{J'} - 4 (\text{Im}(N_{\lambda u}^J N_{\lambda' u}^{J'*}) - \text{Im}(N_{\lambda d}^J N_{\lambda' d}^{J'*})) \text{Im} Y_\lambda^J \text{Im} Y_{\lambda'}^{J'}) \\ I_u^0 &= \sum_{J,\lambda \geq 0} \sum_{J',\lambda' \geq 0} \eta_\lambda \eta_{\lambda'} (\xi_\lambda \xi_{\lambda'} (\text{Re}(U_{\lambda u}^J U_{\lambda' u}^{J'*}) + \text{Re}(U_{\lambda d}^J U_{\lambda' d}^{J'*})) \text{Re} Y_\lambda^J \text{Re} Y_{\lambda'}^{J'} + 4 (\text{Im}(N_{\lambda u}^J N_{\lambda' u}^{J'*}) + \text{Im}(N_{\lambda d}^J N_{\lambda' d}^{J'*})) \text{Im} Y_\lambda^J \text{Im} Y_{\lambda'}^{J'}) \end{aligned} \quad (\text{A2})$$

where $\eta_\lambda = 1$, $\xi_\lambda = 1$ for $\lambda = 0$ and $\eta_\lambda = \frac{1}{\sqrt{2}}$, $\xi_\lambda = 2$ for $\lambda > 0$. Using these expressions the lhs of (A1) reads

$$\begin{aligned} A &= -16 \sum_{J,\lambda \geq 0} \sum_{J',\lambda' \geq 0} \sum_{K,\mu > 0} \sum_{K',\mu' > 0} C_{\lambda\lambda',\mu\mu'} (\text{Re}(U_{\lambda u}^J U_{\lambda' u}^{J'*} N_{\mu u}^K N_{\mu' u}^{K'*}) + \text{Re}(U_{\lambda d}^J U_{\lambda' d}^{J'*} N_{\mu d}^K N_{\mu' d}^{K'*})) \\ &\quad + 2 \text{Re}(U_{\lambda u}^J N_{\mu d}^{K*} U_{\lambda' d}^{J'*} N_{\mu' u}^{K'}) \text{Re} Y_\lambda^J \text{Re} Y_{\lambda'}^{J'} \text{Im} Y_\mu^K \text{Im} Y_{\mu'}^{K'} \end{aligned} \quad (\text{A3})$$

where $C_{\lambda\lambda',\mu\mu'} = \eta_\lambda \eta_{\lambda'} \eta_\mu \eta_{\mu'} \xi_\lambda \xi_{\lambda'} \xi_\mu \xi_{\mu'}$ and where we used some relabeling of dipion spins and helicities and the identities

$$\sum_{J,\lambda \geq 0} \sum_{J',\lambda' \geq 0} \eta_\lambda \eta_{\lambda'} \xi_\lambda \xi_{\lambda'} \text{Im}(U_{\lambda\tau}^J U_{\lambda'\tau}^{J'*}) \text{Re} Y_\lambda^J \text{Re} Y_{\lambda'}^{J'} = 0$$

$$\sum_{K,\mu > 0} \sum_{K',\mu' > 0} \eta_\mu \eta_{\mu'} \xi_\mu \xi_{\mu'} \text{Im}(N_{\mu\tau}^K N_{\mu'\tau}^{K'*}) \text{Im} Y_\mu^K \text{Im} Y_{\mu'}^{K'} = 0. \quad (\text{A4})$$

After a similar procedure the rhs of (A1) can be brought to the form

$$B = A + 16 \sum_{J,\lambda \geq 0} \sum_{J',\lambda' \geq 0} \sum_{K,\mu > 0} \sum_{K',\mu' > 0} C_{\lambda\lambda',\mu\mu'} 4 \text{Im}(U_{\lambda u}^J N_{\mu d}^{K*}) \text{Im}(U_{\lambda' d}^{J'*} N_{\mu' u}^{K'}) \text{Re} Y_\lambda^J \text{Im} Y_\mu^K \text{Re} Y_{\lambda'}^{J'} \text{Im} Y_{\mu'}^{K'}. \quad (\text{A5})$$

Since $A = B$ Eq. (A5) immediately implies the conditions (7.12).

-
- [1] K. Kraus, General state changes in quantum theory, *Ann. Phys. (N.Y.)* **64**, 311 (1971).
- [2] K. Kraus, *States, Effects, and Operations: Fundamental Notions of Quantum Theory*, Lecture Notes in Physics Vol. 190 (Springer-Verlag, Berlin, 1983).
- [3] M. A. Nielsen and I. L. Chuang, *Quantum Computation and Quantum Information* (Cambridge University Press, Cambridge, England, 2000).
- [4] I. Bengtsson and K. Życzkowski, *Geometry of Quantum States—An Introduction to Quantum Entanglement* (Cambridge University Press, Cambridge, England, 2006).
- [5] K. Rybicki (private communication).
- [6] H. Becker *et al.*, Measurement and analysis of reaction $\pi^- p \rightarrow \rho^0 n$ on polarized target, *Nucl. Phys.* **B150**, 301 (1979).
- [7] H. Becker *et al.*, A model independent partial-wave analysis of the $\pi^+\pi^-$ system produced at low four-momentum transfer in the reaction $\pi^- p \uparrow \rightarrow \pi^+\pi^- n$ at 17.2 GeV/c, *Nucl. Phys.* **B151**, 46 (1979).
- [8] V. Chabaud *et al.*, Experimental indications for a 2^{++} non- $\bar{q}q$ object, *Nucl. Phys.* **B223**, 1 (1983).
- [9] K. Rybicki and I. Sakrejda, Indication for a broad $J^{PC} = 2^{++}$ meson at 840 MeV produced in the reaction $\pi^- p \rightarrow \pi^- \pi^+ n$ at high $|t|$, *Z. Phys. C* **28**, 65 (1985).
- [10] M. Svec, A. de Lesquen, and L. van Rossum, Amplitude analysis of reaction $\pi^+ n \rightarrow \pi^+ \pi^- p$ at 5.98 and 11.85 GeV/c, *Phys. Rev. D* **45**, 55 (1992).
- [11] M. Svec, Study of $\sigma(750)$ and $\rho^0(770)$ production in measurements of $\pi N \rightarrow \pi^+ \pi^- N$ on a polarized target at 5.98, 11.85 and 17.2 GeV/c, *Phys. Rev. D* **53**, 2343 (1996).
- [12] M. Svec, Mass and width of the $\sigma(750)$ scalar meson from measurements of $\pi N \rightarrow \pi^- \pi^+ N$ on polarized target, *Phys. Rev. D* **55**, 5727 (1997).
- [13] M. Svec, $\rho^0(770) - f_0(980)$ mixing and CPT violation in a non-unitary evolution of pion creation process $\pi^- p \rightarrow \pi^- \pi^+ n$ on polarized target, [arXiv:0709.0688](https://arxiv.org/abs/0709.0688).
- [14] M. Svec, Determination of S - and P -wave helicity amplitudes and non-unitary evolution of pion creation process $\pi^- p \rightarrow \pi^- \pi^+ n$ on polarized target, [arXiv:0709.2219](https://arxiv.org/abs/0709.2219).
- [15] M. Svec, Evidence for $\rho^0(770) - f_0(980)$ mixing in $\pi^- p \rightarrow \pi^- \pi^+ n$ from CERN measurements on polarized target, [arXiv:1205.6381](https://arxiv.org/abs/1205.6381).
- [16] I. G. Alekseev *et al.* (ITEP Collaboration), Study of the reaction $\pi^- p \rightarrow \pi^- \pi^+ n$ on the polarized proton target at 1.78 GeV/c: Experiment and amplitude analysis, *Nucl. Phys.* **B541**, 3 (1999).
- [17] M. Svec, Study of $\pi N \rightarrow \pi\pi N$ processes on polarized targets: The prediction of $\rho^0(770) - f_0(980)$ spin mixing, [arXiv:1304.5400](https://arxiv.org/abs/1304.5400).
- [18] V. Hagopian and W. Selow, Experimental Evidence on $\pi\pi$ Scattering Near the ρ^0 and f^0 Resonances from $\pi^- + p \rightarrow \pi + \pi + \text{Nucleon}$ at 3 BeV/c, *Phys. Rev. Lett.* **10**, 533 (1963).
- [19] M. M. Islam and R. Pinn, Study of $\pi^- \pi^+$ System in $\pi^- + p \rightarrow \pi^- + \pi^+ + n$ Reaction, *Phys. Rev. Lett.* **12**, 310 (1964).
- [20] S. H. Patil, Analysis of the S -wave in $\pi\pi$ Interactions, *Phys. Rev. Lett.* **13**, 261 (1964).
- [21] L. Durand III and Y. T. Chiu, Decay of the ρ^0 Meson and the Possible Existence of a $T = 0$ Scalar Di-pion, *Phys. Rev. Lett.* **14**, 329 (1965).
- [22] J. P. Baton *et al.*, Single pion production in $\pi^- p$ interactions at 2.75 GeV/c, *Nuovo Cimento* **35**, 713 (1965).
- [23] J. T. Donohue and Y. Leroyer, Is there a narrow ϵ under ρ^0 ? *Nucl. Phys.* **B158**, 123 (1979).
- [24] M. Svec, Consistency tests of $\rho^0(770) - f_0(980)$ mixing in $\pi^- p \rightarrow \pi^- \pi^+ n$, [arXiv:1411.2792](https://arxiv.org/abs/1411.2792).
- [25] M. S. Marinov, A non-Hamiltonian theory of neutral K mesons, *Sov. J. Nucl. Phys.* **19**, 173 (1974).
- [26] R. M. Wald, Quantum gravity and time irreversibility, *Phys. Rev. D* **21**, 2742 (1980).
- [27] S. H. Hawking, The unpredictability of quantum gravity, *Commun. Math. Phys.* **87**, 395 (1982).
- [28] S. H. Hawking, Non-trivial topologies in quantum gravity, *Nucl. Phys.* **B244**, 135 (1984).
- [29] W. G. Unruh and R. M. Wald, On evolution laws taking pure states to mixed states in quantum field theory, *Phys. Rev. D* **52**, 2176 (1995).
- [30] J. Oppenheim and B. Reznik, Fundamental destruction of information and conservation laws, [arXiv:0902.2361](https://arxiv.org/abs/0902.2361).

- [31] O. W. Greenberg, *CPT Violation Implies Violation of Lorentz Symmetry*, *Phys. Rev. Lett.* **89**, 231602 (2002).
- [32] J. Ellis, J. S. Hagelin, D. V. Nanopoulos, and M. Srednicki, Search for violations of quantum mechanics, *Nucl. Phys.* **B241**, 381 (1984).
- [33] J. Ellis, J. L. Lopez, N. E. Mavromatos, and D. V. Nanopoulos, Precision tests of *CPT* symmetry and quantum mechanics in the neutral kaon system, *Phys. Rev. D* **53**, 3846 (1996).
- [34] P. Huet and M. E. Peskin, Violations of *CPT* and quantum mechanics in the $K^0\bar{K}^0$ system, *Nucl. Phys.* **B434**, 3 (1995).
- [35] F. Benatti and R. Floreanini, Completely positive dynamical maps and the neutral kaon system, *Nucl. Phys.* **B488**, 335 (1997).
- [36] H.-J. Gerber, Searching for Evolution from Pure States into Mixed States in the Two-State System $K^0\bar{K}^0$, *Phys. Rev. Lett.* **80**, 2969 (1998).
- [37] H.-J. Gerber, Searching for evolution from pure states into mixed states with entangled neutral kaons, *Eur. Phys. J. C* **32**, 229 (2004).
- [38] J. Bernabéu, N. E. Mavromatos, and S. Sarkar, Decoherence induced *CPT* violation and entangled neutral mesons, *Phys. Rev. D* **74**, 045014 (2006).
- [39] J. Bernabéu, J. Ellis, N. E. Mavromatos, D. V. Nanopoulos, and J. Papavassiliou, *CPT* and quantum mechanics tests with kaons, [arXiv:hep-ph/0607322](https://arxiv.org/abs/hep-ph/0607322).
- [40] M. Fidecaro and H.-J. Gerber, The fundamental symmetries in the neutral kaon system, *Rep. Prog. Phys.* **69**, 1713 (2006).
- [41] F. Ambrosino *et al.* (KLOE Collaboration), First observation of quantum interference in the process $\phi \rightarrow K_S K_L \rightarrow \pi^+ \pi^- \pi^+ \pi^-$: Test of quantum mechanics and *CPT* theorem, *Phys. Lett. B* **642**, 315 (2006).
- [42] G. Amelino-Camelia *et al.* (KLOE Collaboration), Physics with the KLOE-2 experiment at the upgraded DAΦNE, *Eur. Phys. J. C* **68**, 619 (2010).
- [43] R. F. Streater and A. S. Wightman, *PCT, Spin and Statistics, and All That* (Princeton University Press, Princeton, NJ, 1980).
- [44] R. G. Sachs, *The Physics of Time Reversal* (University of Chicago Press, Chicago, 1987).
- [45] A. D. Martin and T. D. Spearman, *Elementary Particle Theory* (North-Holland, Amsterdam, 1970).
- [46] M. Jacob and G. C. Wick, On the general theory of collisions for particles with spin, *Ann. Phys. (N.Y.)* **7**, 404 (1959).
- [47] M. L. Perl, *High Energy Hadron Physics* (Wiley, New York, 1974).
- [48] G. C. Wick, Angular momentum states for three particles, *Ann. Phys. (N.Y.)* **18**, 65 (1962).
- [49] A. R. Edmonds, *Angular Momentum in Quantum Mechanics* (Princeton University Press, Princeton, NJ, 1957).
- [50] E. Leader, *Spin in Particle Physics* (Cambridge University Press, Cambridge, England, 2001).
- [51] G. Lutz and K. Rybicki, Max Planck Institute for Physics and Astrophysics Report No. MPI-PAE/Exp.El.75, 1978 (unpublished).
- [52] C. Bourrely, E. Leader, and J. Soffer, Polarization phenomena in hadronic reactions, *Phys. Rep.* **59**, 95 (1980).
- [53] M. Svec, Spin mixing mechanism in amplitude analysis of $\pi^- p \rightarrow \pi^- \pi^+ n$ and a new view of dark matter, [arXiv:1411.4468](https://arxiv.org/abs/1411.4468).
- [54] G. Grayer *et al.*, High statistics study of the reaction $\pi^- p \rightarrow \pi^- \pi^+ n$: Apparatus, method of analysis, and general features of results at 17.2 GeV/c, *Nucl. Phys.* **B75**, 189 (1974).
- [55] M. Svec, Evidence for a non-unitary evolution law in $\pi^- p \rightarrow \pi^- \pi^+ n$ (unpublished).
- [56] J. Gunter *et al.* (BNL E852 Collaboration), Partial wave analysis of the $\pi^0 \pi^0$ system produced in $\pi^- p$ charge exchange collisions, *Phys. Rev. D* **64**, 072003 (2001).
- [57] X. Shi and G. M. Fuller, A New Dark Matter Candidate: Non-Thermal Sterile Neutrino, *Phys. Rev. Lett.* **82**, 2832 (1999).
- [58] K. N. Abazajian and G. M. Fuller, Bulk QCD thermodynamics and sterile neutrino dark matter, *Phys. Rev. D* **66**, 023526 (2002).
- [59] K. Abazajian, G. M. Fuller, and W. H. Tucker, Direct detection of warm dark matter in the x-ray, *Astrophys. J.* **562**, 593 (2001).
- [60] K. N. Abazajian, Resonantly Produced 7 keV Sterile Neutrino Dark Matter Models and the Properties of Milky Way Satellites, *Phys. Rev. Lett.* **112**, 161303 (2014).
- [61] E. Bulbul, M. Markevitch, A. Foster, R. K. Smith, M. Loewenstein, and S. W. Randall, Detection of an unidentified emission line in the stacked x-ray spectrum of galaxy clusters, *Astrophys. J.* **789**, 13 (2014).
- [62] A. Boyarski, O. Ruchayskiy, D. Iakubovskiy, and J. Franse, An Unidentified Line in X-Ray Spectra of the Andromeda Galaxy and Perseus Galaxy Cluster, *Phys. Rev. Lett.* **113**, 251301 (2014).